Influence of ligand substitution and solvent effect on structures and magnetic properties of dinuclear Dy_2 supramolecular architectures constructed with bis-*β*-diketonate-Dy_2 building block as metalloligand

Jiamin Tang,[a] Sheng Zhang,[*a] Linzhou Li,[a] Linbin Yao,[a] Ronghu Zhang,[*b,c] Bing Yin,[*d] Jiangwei Zhang[*e]

AUTHOR ADDRESS

[a.] *School of Science, Hainan University, Haikou 570228, China*

[b.] *Key Laboratory of Tropical Biological Resources of Ministry of Education, Hainan University, Haikou 570228, China*

[c.] *Institute of Processing&Design of Agroproducts, Hainan Academy of Agricultural Science, Haikou 571100, China*

[d.] *Lab of Theoretical Molecular Magnetism (LTMM), College of Chemistry and Materials Science, Northwest University, Xi'an, 710127 P. R. China*

[e.] *Zhang Dayu College of Chemistry, State Key Laboratory of Fine Chemicals, Dalian University of Technology, Dalian 116024, P. R. China Dalian National Laboratory for Clean Energy & State Key Laboratory of Catalysis, Dalian Institute of Chemical Physics, Chinese Academy of Sciences, Dalian, 116023, P. R. China*

Corresponding authors

***E-mail: zhangsheng19890501@163.com (S. Zhang)**

***E-mail: zrh0912@ 126.com (R. H. Zhang)**

***E-mail: rayinyin@nwu.edu.cn (B. Yin)**

***E-mail: zjw11@tsinghua.org.cn (J. W. Zhang)**

Table S1 Bond lengths and bond angles for **1-6**.

Compound **1**		
Atom	**Atom**	**Length/Å**
Dy1	O3	2.330(7)
Dy1	O4	2.342(8)
Dy1	O7	2.321(7)
Dy1	O8	2.346(8)
Dy1	O11	2.315(8)
Dy1	O12	2.398(7)
Dy1	O15	2.337(7)
Dy1	O16	2.363(8)
Dy2	O1	2.361(8)
Dy2	O2	2.329(7)
Dy2	O5	2.338(8)
Dy2	O6	2.328(7)
Dy2	O9	2.352(8)
Dy2	O10	2.317(8)
Dy2	O13	2.394(7)
Dy2	O14	2.354(7)

Atom	**Atom**	**Atom**	**Angle/°**
O3	Dy1	O4	74.3(3)
O3	Dy1	O8	80.3(3)
O3	Dy1	O12	147.5(3)
O3	Dy1	O15	71.3(2)
O3	Dy1	O16	137.2(2)
O4	Dy1	O8	73.3(3)
O4	Dy1	O12	117.2(3)
O4	Dy1	O16	77.5(3)
O7	Dy1	O3	73.7(3)
O7	Dy1	O4	137.2(3)
O7	Dy1	O8	74.0(3)
O7	Dy1	O12	79.3(3)
O7	Dy1	O15	114.2(3)
O7	Dy1	O16	144.2(3)
O8	Dy1	O12	75.1(3)
O8	Dy1	O16	121.0(3)
O11	Dy1	O3	112.6(3)
O11	Dy1	O4	148.1(3)
O11	Dy1	O7	71.9(3)

O11	Dy1	O8	137.6(3)
O11	Dy1	O12	74.6(3)
O11	Dy1	O15	73.0(3)
O11	Dy1	O16	77.8(3)
O15	Dy1	O4	80.8(3)
O15	Dy1	O8	145.7(3)
O15	Dy1	O12	138.0(3)
O15	Dy1	O16	73.0(3)
O16	Dy1	O12	74.7(3)
O1	Dy2	O13	74.2(3)
O2	Dy2	O1	73.5(3)
O2	Dy2	O5	137.5(3)
O2	Dy2	O9	147.0(3)
O2	Dy2	O13	81.3(3)
O2	Dy2	O14	72.1(3)
O5	Dy2	O1	75.9(3)
O5	Dy2	O9	74.8(3)
O5	Dy2	O13	117.5(3)
O5	Dy2	O14	146.9(3)
O6	Dy2	O1	80.1(3)
O6	Dy2	O2	72.6(3)
O6	Dy2	O5	73.7(3)
O6	Dy2	O9	136.4(3)
O6	Dy2	O13	147.5(3)
O6	Dy2	O14	113.9(3)
O9	Dy2	O1	119.8(3)
O9	Dy2	O13	74.8(3)
O9	Dy2	O14	79.6(3)
O10	Dy2	O1	148.4(3)
O10	Dy2	O2	111.1(3)
O10	Dy2	O5	81.7(3)
O10	Dy2	O6	72.3(3)
O10	Dy2	O9	74.1(3)
O10	Dy2	O13	136.9(3)
O10	Dy2	O14	71.2(3)
O14	Dy2	O1	136.1(3)
O14	Dy2	O13	74.4(3)
Compound **2**			

Atom	Atom	Length/Å
Dy1	N1	2.533(8)
Dy1	N2	2.551(10)
Dy1	O1	2.321(9)
Dy1	O2	2.366(7)
Dy1	O3[1]	2.311(7)
Dy1	O4[1]	2.327(8)
Dy1	O5	2.315(9)
Dy1	O6	2.362(7)

[1]-X,-Y,+Z

Atom	Atom	Atom	Angle/°
N1	Dy1	N2	64.9(4)
O1	Dy1	N1	69.9(5)
O1	Dy1	N2	105.0(3)
O1	Dy1	O2	73.7(3)
O1	Dy1	O4[1]	75.6(3)
O1	Dy1	O6	154.1(3)
O2	Dy1	N1	113.8(3)
O2	Dy1	N2	74.2(3)
O3[1]	Dy1	N1	146.7(4)
O3[1]	Dy1	N2	144.3(3)
O3[1]	Dy1	O1	83.3(3)
O3[1]	Dy1	O2	75.2(2)
O3[1]	Dy1	O4[1]	73.4(3)
O3[1]	Dy1	O5	121.7(3)
O3[1]	Dy1	O6	79.5(3)
O4[1]	Dy1	N1	80.7(3)
O4[1]	Dy1	N2	142.2(3)
O4[1]	Dy1	O2	138.0(3)
O4[1]	Dy1	O6	117.1(3)
O5	Dy1	N1	69.8(5)
O5	Dy1	N2	77.7(3)
O5	Dy1	O1	133.4(3)
O5	Dy1	O2	145.7(3)
O5	Dy1	O4[1]	75.8(3)
O5	Dy1	O6	72.4(3)
O6	Dy1	N1	132.1(5)
O6	Dy1	N2	79.2(3)
O6	Dy1	O2	83.2(2)

[1]-X,-Y,+Z

Compound **3**

Atom	Atom	Length/Å
Dy1	N1	2.534(6)
Dy1	N2	2.567(7)
Dy1	O1	2.308(6)
Dy1	O2	2.315(6)
Dy1	O5	2.336(6)
Dy1	O6	2.310(5)
Dy1	O9	2.335(6)
Dy1	O10	2.350(6)
Dy2	N3	2.543(8)
Dy2	N4	2.537(7)
Dy2	O3	2.361(6)
Dy2	O4	2.328(7)
Dy2	O7	2.303(6)
Dy2	O8	2.298(7)
Dy2	O11	2.327(5)
Dy2	O12	2.311(6)

Atom	Atom	Atom	Angle/°
N1	Dy1	N2	63.9(2)
O1	Dy1	N1	79.5(2)
O1	Dy1	N2	136.9(2)
O1	Dy1	O2	73.9(2)
O1	Dy1	O5	77.7(2)
O1	Dy1	O6	142.5(2)
O1	Dy1	O9	75.3(2)
O1	Dy1	O10	119.5(2)
O2	Dy1	N1	146.3(2)
O2	Dy1	N2	148.0(2)
O2	Dy1	O5	84.2(2)
O2	Dy1	O9	116.5(2)
O2	Dy1	O10	76.37(19)
O5	Dy1	N1	70.0(2)
O5	Dy1	N2	107.9(2)
O5	Dy1	O10	148.04(19)
O6	Dy1	N1	109.6(2)
O6	Dy1	N2	74.9(2)

O6	Dy1	O2	81.26(19)
O6	Dy1	O5	72.1(2)
O6	Dy1	O9	141.9(2)
O6	Dy1	O10	79.93(19)
O9	Dy1	N1	75.0(2)
O9	Dy1	N2	73.9(2)
O9	Dy1	O5	139.0(2)
O9	Dy1	O10	72.9(2)
O10	Dy1	N1	136.0(2)
O10	Dy1	N2	78.7(2)
N4	Dy2	N3	63.0(3)
O3	Dy2	N3	128.0(2)
O3	Dy2	N4	77.0(2)
O4	Dy2	N3	70.8(3)
O4	Dy2	N4	82.2(2)
O4	Dy2	O3	72.1(2)
O7	Dy2	N3	113.2(3)
O7	Dy2	N4	72.7(2)
O7	Dy2	O3	82.30(19)
O7	Dy2	O4	147.5(2)
O7	Dy2	O11	77.2(2)
O7	Dy2	O12	137.1(2)
O8	Dy2	N3	73.0(3)
O8	Dy2	N4	104.2(2)
O8	Dy2	O3	152.9(2)
O8	Dy2	O4	135.0(2)
O8	Dy2	O7	72.6(2)
O8	Dy2	O11	87.1(2)
O8	Dy2	O12	75.0(2)
O11	Dy2	N3	152.5(2)
O11	Dy2	N4	142.6(2)
O11	Dy2	O3	77.42(19)
O11	Dy2	O4	114.8(2)
O12	Dy2	N3	82.7(3)
O12	Dy2	N4	143.5(2)
O12	Dy2	O3	120.3(2)
O12	Dy2	O4	74.6(2)
O12	Dy2	O11	73.7(2)

Compound **4**		
Atom	**Atom**	**Length/Å**
Dy1	N1	2.583(4)
Dy1	N2	2.582(4)
Dy1	O1	2.348(4)
Dy1	O2	2.333(3)
Dy1	O3[1]	2.308(3)
Dy1	O4[1]	2.316(4)
Dy1	O5	2.344(3)
Dy1	O6	2.285(3)

[1]-X,+Y,1/2+Z

Atom	**Atom**	**Atom**	**Angle/°**
N2	Dy1	N1	63.03(12)
O1	Dy1	N1	70.77(14)
O1	Dy1	N2	94.40(14)
O2	Dy1	N1	117.26(13)
O2	Dy1	N2	72.37(11)
O2	Dy1	O1	71.22(12)
O2	Dy1	O5	77.15(11)
O3[1]	Dy1	N1	127.24(13)
O3[1]	Dy1	N2	77.38(13)
O3[1]	Dy1	O1	149.36(11)
O3[1]	Dy1	O2	78.18(11)
O3[1]	Dy1	O4[1]	71.78(12)
O3[1]	Dy1	O5	76.72(11)
O4[1]	Dy1	N1	69.21(14)
O4[1]	Dy1	N2	81.47(13)
O4[1]	Dy1	O1	136.86(12)
O4[1]	Dy1	O2	143.71(13)
O4[1]	Dy1	O5	114.05(13)
O5	Dy1	N1	152.65(12)
O5	Dy1	N2	143.26(11)
O5	Dy1	O1	94.76(13)
O6	Dy1	N1	80.29(12)

O6	Dy1	N2	143.23(12)
O6	Dy1	O1	74.75(14)
O6	Dy1	O2	132.30(13)
O6	Dy1	O3[1]	128.31(13)
O6	Dy1	O4[1]	83.26(14)
O6	Dy1	O5	73.41(11)

[1]-X,+Y,1/2+Z

Compound **4a**

Atom	**Atom**	**Length/Å**
Dy1	N1	2.565(7)
Dy1	N2	2.572(7)
Dy1	O1	2.283(5)
Dy1	O2	2.331(4)
Dy1	O5	2.325(7)
Dy1	O6	2.304(6)
Dy1	O9	2.328(5)
Dy1	O10	2.343(5)
Dy2	N5	2.556(7)
Dy2	N6	2.502(7)
Dy2	O3	2.336(6)
Dy2	O4	2.266(6)
Dy2	O7	2.294(6)
Dy2	O8	2.347(9)
Dy2	O11	2.277(7)
Dy2	O12	2.388(8)

Atom	**Atom**	**Atom**	**Angle/°**
N1	Dy1	N2	62.8(2)
O1	Dy1	N1	83.1(2)
O1	Dy1	N2	145.33(19)
O1	Dy1	O2	73.75(18)
O1	Dy1	O5	73.8(2)
O1	Dy1	O6	133.11(19)
O1	Dy1	O9	81.57(19)
O1	Dy1	O10	122.23(19)
O2	Dy1	N1	153.3(2)
O2	Dy1	N2	140.8(2)
O2	Dy1	O10	78.86(18)
O5	Dy1	N1	71.0(2)
O5	Dy1	N2	99.0(2)

O5	Dy1	O2	89.6(2)
O5	Dy1	O9	132.4(2)
O5	Dy1	O10	155.4(2)
O6	Dy1	N1	113.9(2)
O6	Dy1	N2	71.6(2)
O6	Dy1	O2	75.07(19)
O6	Dy1	O5	71.84(18)
O6	Dy1	O9	145.21(19)
O6	Dy1	O10	84.2(2)
O9	Dy1	N1	66.0(2)
O9	Dy1	N2	79.1(2)
O9	Dy1	O2	121.80(18)
O9	Dy1	O10	71.4(2)
O10	Dy1	N1	125.9(2)
O10	Dy1	N2	77.8(2)
N6	Dy2	N5	64.2(2)
O3	Dy2	N5	138.6(2)
O3	Dy2	N6	151.0(2)
O3	Dy2	O8	122.8(3)
O3	Dy2	O12	81.7(2)
O4	Dy2	N5	146.8(2)
O4	Dy2	N6	88.2(2)
O4	Dy2	O3	74.0(2)
O4	Dy2	O7	111.3(3)
O4	Dy2	O8	75.1(3)
O4	Dy2	O11	139.9(3)
O4	Dy2	O12	76.4(3)
O7	Dy2	N5	79.2(2)
O7	Dy2	N6	132.8(2)
O7	Dy2	O3	75.9(2)
O7	Dy2	O8	72.4(2)
O7	Dy2	O12	152.7(2)
O8	Dy2	N5	78.8(3)
O8	Dy2	N6	72.1(3)
O8	Dy2	O12	134.1(3)
O11	Dy2	N5	68.9(3)
O11	Dy2	N6	104.1(3)
O11	Dy2	O3	77.8(2)
O11	Dy2	O7	88.2(2)

O11	Dy2	O8	144.9(3)
O11	Dy2	O12	71.8(3)
O12	Dy2	N5	109.2(3)
O12	Dy2	N6	71.8(3)

Compound **5**

Atom	**Atom**	**Length/Å**
Dy1	N1	2.541(3)
Dy1	N2	2.528(3)
Dy1	O1	2.348(2)
Dy1	O2	2.337(2)
Dy1	O3[1]	2.300(2)
Dy1	O4[1]	2.334(2)
Dy1	O5	2.316(2)
Dy1	O6	2.352(2)

[1]-X,+Y,1/2+Z

Atom	**Atom**	**Atom**	**Angle/°**
N2	Dy1	N1	63.64(8)
O1	Dy1	N1	70.90(9)
O1	Dy1	N2	107.85(9)
O1	Dy1	O6	149.04(8)
O2	Dy1	N1	110.75(8)
O2	Dy1	N2	74.88(9)
O2	Dy1	O1	72.75(8)
O2	Dy1	O6	81.76(7)
O3[1]	Dy1	N1	146.56(8)
O3[1]	Dy1	N2	147.24(8)
O3[1]	Dy1	O1	82.79(10)
O3[1]	Dy1	O2	79.26(9)
O3[1]	Dy1	O4[1]	72.95(8)
O3[1]	Dy1	O5	118.01(9)
O3[1]	Dy1	O6	75.33(8)
O4[1]	Dy1	N1	80.26(8)
O4[1]	Dy1	N2	139.36(8)
O4[1]	Dy1	O1	74.62(9)
O4[1]	Dy1	O2	139.21(8)
O4[1]	Dy1	O6	118.00(8)
O5	Dy1	N1	73.52(8)
O5	Dy1	N2	75.38(8)
O5	Dy1	O1	137.43(8)

O5	Dy1	O2	143.44(8)
O5	Dy1	O4[1]	77.04(8)
O5	Dy1	O6	73.15(7)
O6	Dy1	N1	136.43(8)
O6	Dy1	N2	81.31(8)

[1]-X,+Y,1/2+Z

Compound **6**

Atom	**Atom**	**Length/Å**
Dy1	N1	2.538(6)
Dy1	N2	2.547(5)
Dy1	O1	2.340(5)
Dy1	O2	2.385(4)
Dy1	O5	2.290(5)
Dy1	O6	2.305(4)
Dy1	O9	2.345(5)
Dy1	O10	2.315(4)
Dy2	N3	2.534(5)
Dy2	N4	2.523(6)
Dy2	O3	2.298(5)
Dy2	O4	2.291(5)
Dy2	O7	2.349(4)
Dy2	O8	2.342(6)
Dy2	O11	2.338(5)
Dy2	O12	2.309(6)

Atom	**Atom**	**Atom**	**Angle/°**
N1	Dy1	N2	63.68(19)
O1	Dy1	N1	71.20(19)
O1	Dy1	N2	114.18(19)
O1	Dy1	O2	72.79(17)
O1	Dy1	O9	131.49(18)
O2	Dy1	N1	104.13(19)
O2	Dy1	N2	74.73(15)
O5	Dy1	N1	88.3(2)
O5	Dy1	N2	141.89(17)
O5	Dy1	O1	76.3(2)
O5	Dy1	O2	140.51(16)
O5	Dy1	O6	73.56(16)
O5	Dy1	O9	72.60(18)
O5	Dy1	O10	109.43(18)

O6	Dy1	N1	150.40(18)
O6	Dy1	N2	142.03(15)
O6	Dy1	O1	81.71(18)
O6	Dy1	O2	78.13(15)
O6	Dy1	O9	122.26(18)
O6	Dy1	O10	76.08(16)
O9	Dy1	N1	71.6(2)
O9	Dy1	N2	74.16(17)
O9	Dy1	O2	146.87(15)
O10	Dy1	N1	132.94(17)
O10	Dy1	N2	77.57(16)
O10	Dy1	O1	154.01(16)
O10	Dy1	O2	89.41(15)
O10	Dy1	O9	73.02(16)
N4	Dy2	N3	63.35(18)
O3	Dy2	N3	138.71(16)
O3	Dy2	N4	157.16(18)
O3	Dy2	O7	75.73(15)
O3	Dy2	O8	92.31(19)
O3	Dy2	O11	78.19(17)
O3	Dy2	O12	108.9(2)
O4	Dy2	N3	147.98(18)
O4	Dy2	N4	85.22(19)
O4	Dy2	O3	73.25(17)
O4	Dy2	O7	130.8(2)
O4	Dy2	O8	72.5(2)
O4	Dy2	O11	122.1(2)
O4	Dy2	O12	71.1(3)
O7	Dy2	N3	72.71(16)
O7	Dy2	N4	114.95(17)
O8	Dy2	N3	102.15(19)
O8	Dy2	N4	73.6(2)
O8	Dy2	O7	71.63(16)
O11	Dy2	N3	74.17(17)
O11	Dy2	N4	120.98(19)
O11	Dy2	O7	86.81(15)
O11	Dy2	O8	158.08(17)
O12	Dy2	N3	91.2(2)
O12	Dy2	N4	69.8(2)

O12	Dy2	O7	156.7(2)
O12	Dy2	O8	129.6(2)
O12	Dy2	O11	72.33(19)

Table S2 The distances and angles between Dy(III) ions.

	The intramolecular distances between Dy(III) ions, Dy···Dy (Å)	The intermolecular distances between Dy(III) ions, Dy···Dy (Å)	The angles of Dy-L-Dy (°)
1	7.5495(11)	10.7388(12)/20.0870(12)	79.629(9)
2	8.1410(6)	16.6783(14)	86.191(7)
3	8.0983(11)	10.0834(10)/13.9362(14)	86.045(11)
4	8.1673(6)	11.2574(8)/14.3113(6)	86.167(6)
4a	7.9012(8)	11.8914(8)/11.7990(10)/11.8914（10）	83.876(8)
5	8.0712(11)	9.6058(6)/13.0524(11)	84.543(4)
6	7.9973(7)	10.5124(7)/17.3209(7)	84.072(6)

Table S3 Dy^{III} ion geometry analysis by SHAPE 2.1 software.

Configuration	**1**		**2**	
	Dy1	**Dy2**	**Dy1**	**Dy1A**
Octagon (D_{8h})	28.079	28.660	29.750	29.750
Heptagonal pyramid (C_{7v})	23.666	23.925	22.935	22.935
Hexagonal bipyramid (D_{6h})	15.754	15.549	14.544	14.544
Cube (O_h)	8.465	7.896	8.106	8.106
Square antiprism (D_{4d})	0.278	0.362	0.616	0.616
Triangular dodecahedron (D_{2d})	2.197	1.907	2.147	2.147
Johnson gyrobifastigium J26 (D_{2d})	15.786	16.140	15.172	15.172
Johnson elongated triangular bipyramid J14 (D_{3h})	28.640	29.011	28.185	28.185
Biaugmented trigonal prism J50 (C_{2v})	2.856	2.814	2.600	2.600
Biaugmented trigonal prism (C_{2v})	2.042	2.032	2.038	2.038
Snub diphenoid J84 (D_{2d})	5.346	5.062	5.224	5.224
Triakis tetrahedron (T_d)	9.275	8.767	8.778	8.778
Elongated trigonal bipyramid (D_{3h})	23.759	23.948	23.747	23.747
Configuration	**3**		**4**	
	Dy1	**Dy2**	**Dy1**	**Dy1A**
Octagon (D_{8h})	30.249	30.868	31.239	31.239
Heptagonal pyramid (C_{7v})	22.179	23.142	22.297	22.297
Hexagonal bipyramid (D_{6h})	16.485	14.012	14.741	14.741
Cube (O_h)	9.943	7.133	7.825	7.825
Square antiprism (D_{4d})	0.413	0.919	1.695	1.695
Triangular dodecahedron (D_{2d})	2.424	1.455	0.827	0.827
Johnson gyrobifastigium J26 (D_{2d})	16.543	15.746	15.366	15.366

Johnson elongated triangular bipyramid J14 (D_{3h})	27.856	28.371	27.036	27.036
Biaugmented trigonal prism J50 (C_{2v})	3.067	2.936	2.543	2.543
Biaugmented trigonal prism (C_{2v})	2.397	2.286	1.859	1.859
Snub diphenoid J84 (D_{2d})	5.423	4.831	4.026	4.026
Triakis tetrahedron (T_d)	10.746	7.916	8.680	8.680
Elongated trigonal bipyramid (D_{3h})	23.993	23.939	23.702	23.702

Configuration	**4a**		**5**	
	Dy1	**Dy2**	**Dy1**	**Dy1A**
Octagon (D_{8h})	30.494	31.924	30.096	30.096
Heptagonal pyramid (C_{7v})	22.433	22.979	21.717	21.717
Hexagonal bipyramid (D_{6h})	13.495	14.085	16.114	16.114
Cube (O_h)	6.744	7.199	9.274	9.274
Square antiprism (D_{4d})	1.338	0.996	0.438	0.438
Triangular dodecahedron (D_{2d})	1.637	1.409	2.386	2.386
Johnson gyrobifastigium J26 (D_{2d})	14.647	15.857	16.958	16.958
Johnson elongated triangular bipyramid J14 (D_{3h})	26.327	28.500	28.457	28.457
Biaugmented trigonal prism J50 (C_{2v})	2.827	2.977	2.922	2.922
Biaugmented trigonal prism (C_{2v})	2.031	2.592	2.362	2.362
Snub diphenoid J84 (D_{2d})	5.189	4.355	5.333	5.333
Triakis tetrahedron (T_d)	7.547	7.907	9.954	9.954
Elongated trigonal bipyramid (D_{3h})	22.800	24.353	24.127	24.127

Configuration	**6**	
	Dy1	**Dy2**
Octagon (D_{8h})	31.380	32.895
Heptagonal pyramid (C_{7v})	22.712	23.471
Hexagonal bipyramid (D_{6h})	14.702	11.680
Cube (O_h)	7.569	4.771
Square antiprism (D_{4d})	0.993	2.231
Triangular dodecahedron (D_{2d})	1.085	1.099
Johnson gyrobifastigium J26 (D_{2d})	16.482	15.651
Johnson elongated triangular bipyramid J14 (D_{3h})	28.131	27.597
Biaugmented trigonal prism J50 (C_{2v})	2.961	4.041
Biaugmented trigonal prism (C_{2v})	2.296	3.499
Snub diphenoid J84 (D_{2d})	4.280	5.019
Triakis tetrahedron (T_d)	8.318	5.626
Elongated trigonal bipyramid (D_{3h})	23.888	24.396

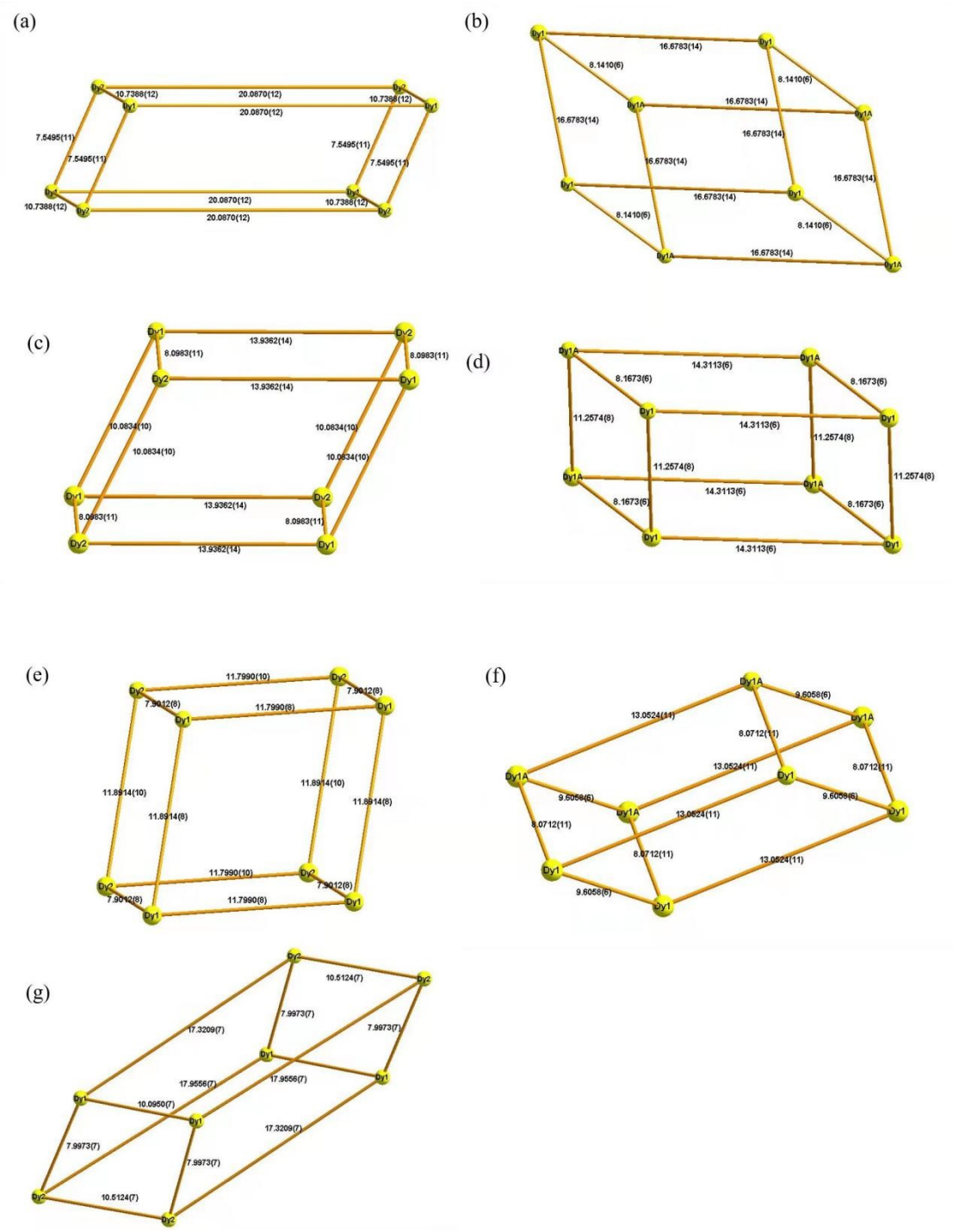

Figure S1. The intermolecular distances of Dy^{III} units in **1-6** (a-g).

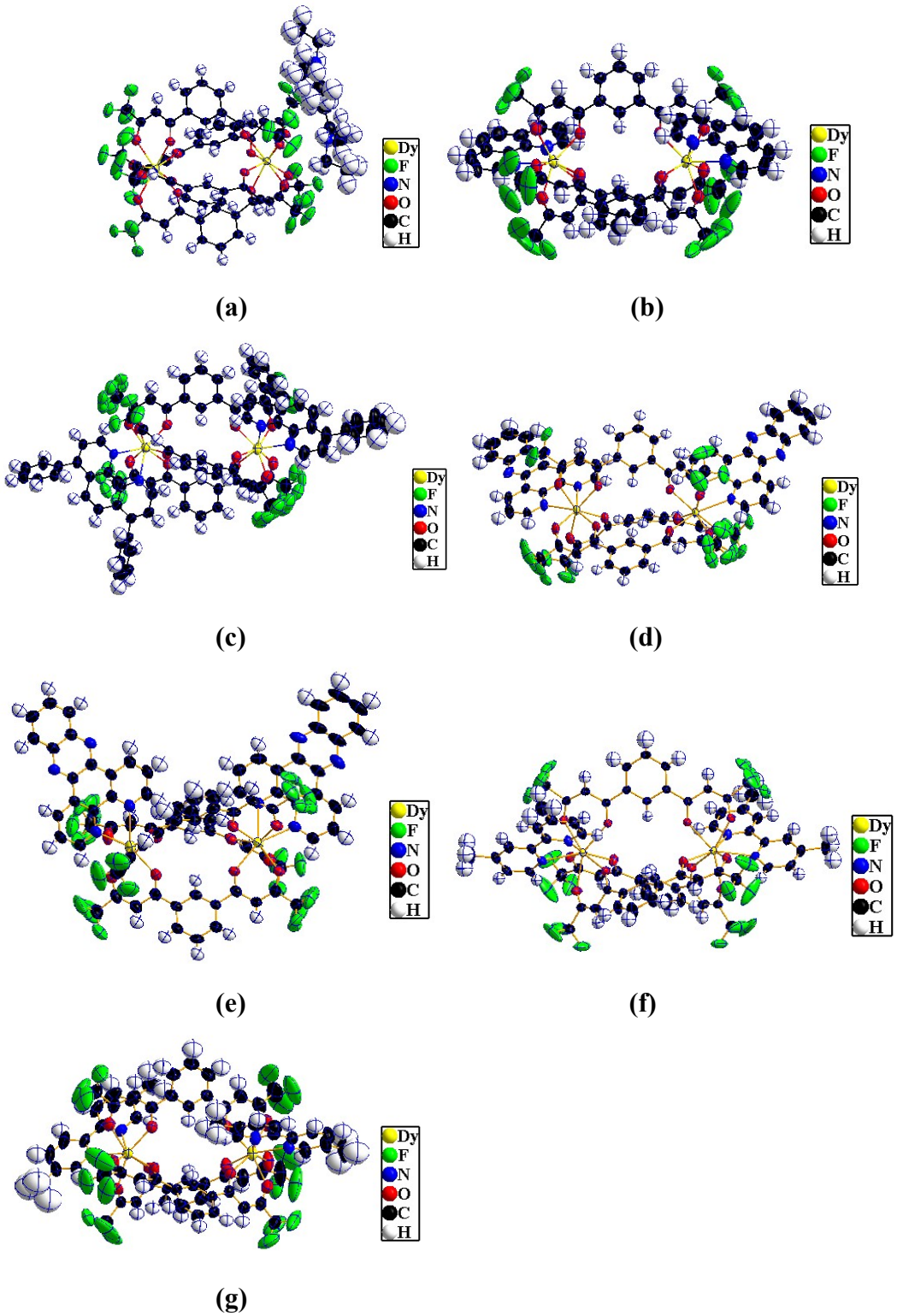

Figure S2. The asymmetric units of **1**-**6** (a-g) with the thermal ellipsoids for non-hydrogen atoms.

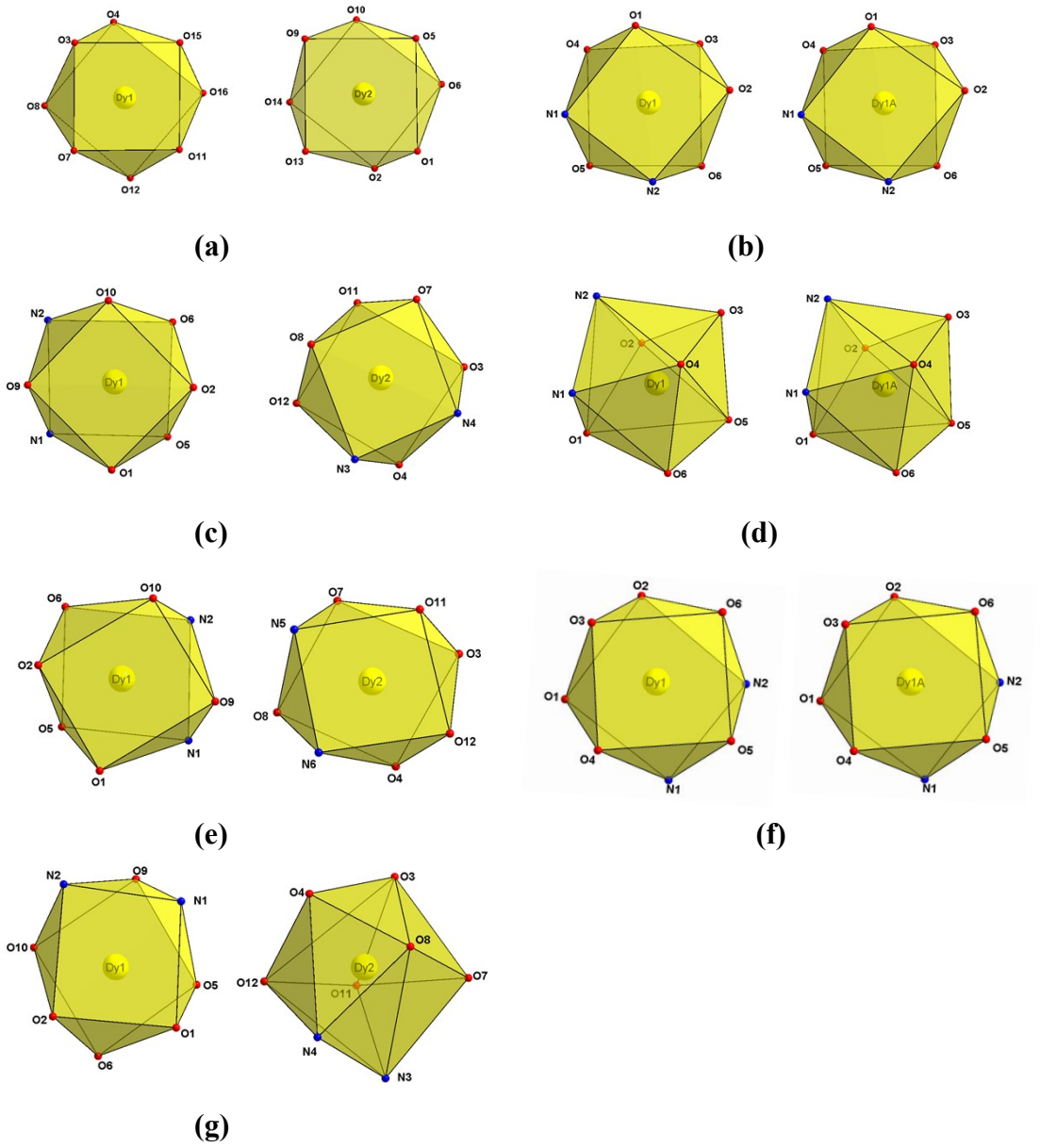

Figure S3. Local coordination geometries of the Dy ^{III} ions for **1-6** (a-g)**.**

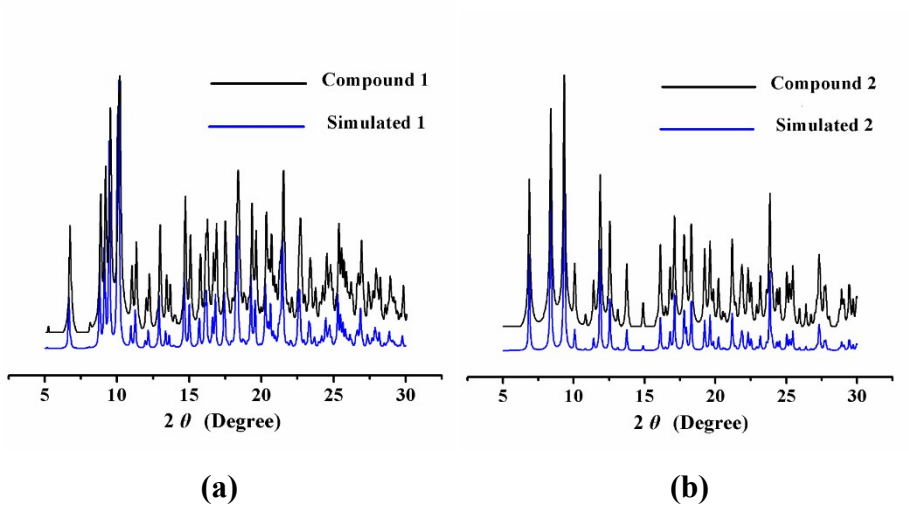

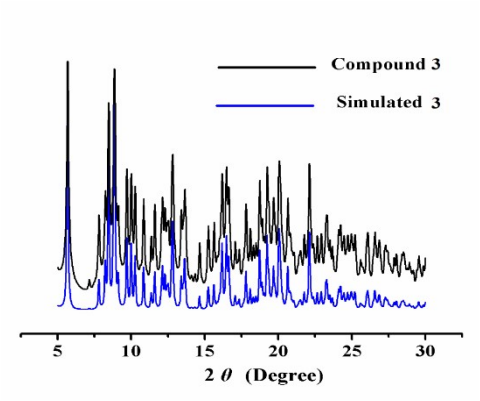

(c)

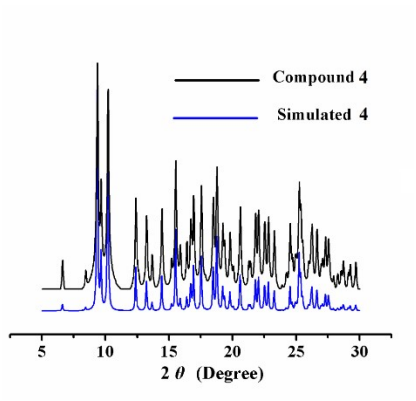

(d)

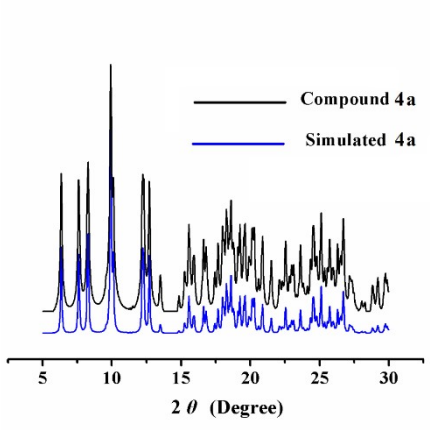

(e)

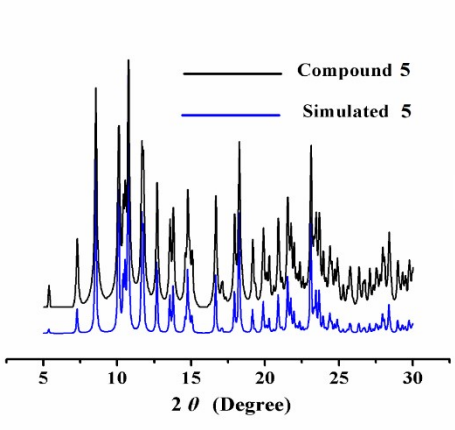

(f)

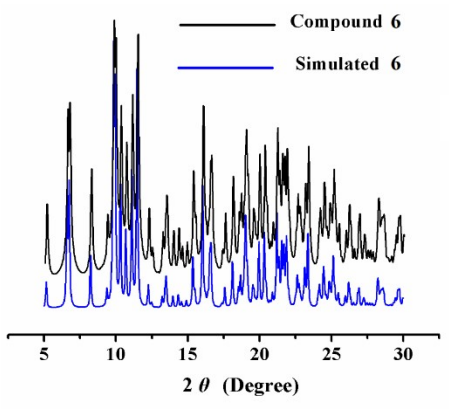

(g)

Figure S4. PXRD curves of **1-6** (a-g).

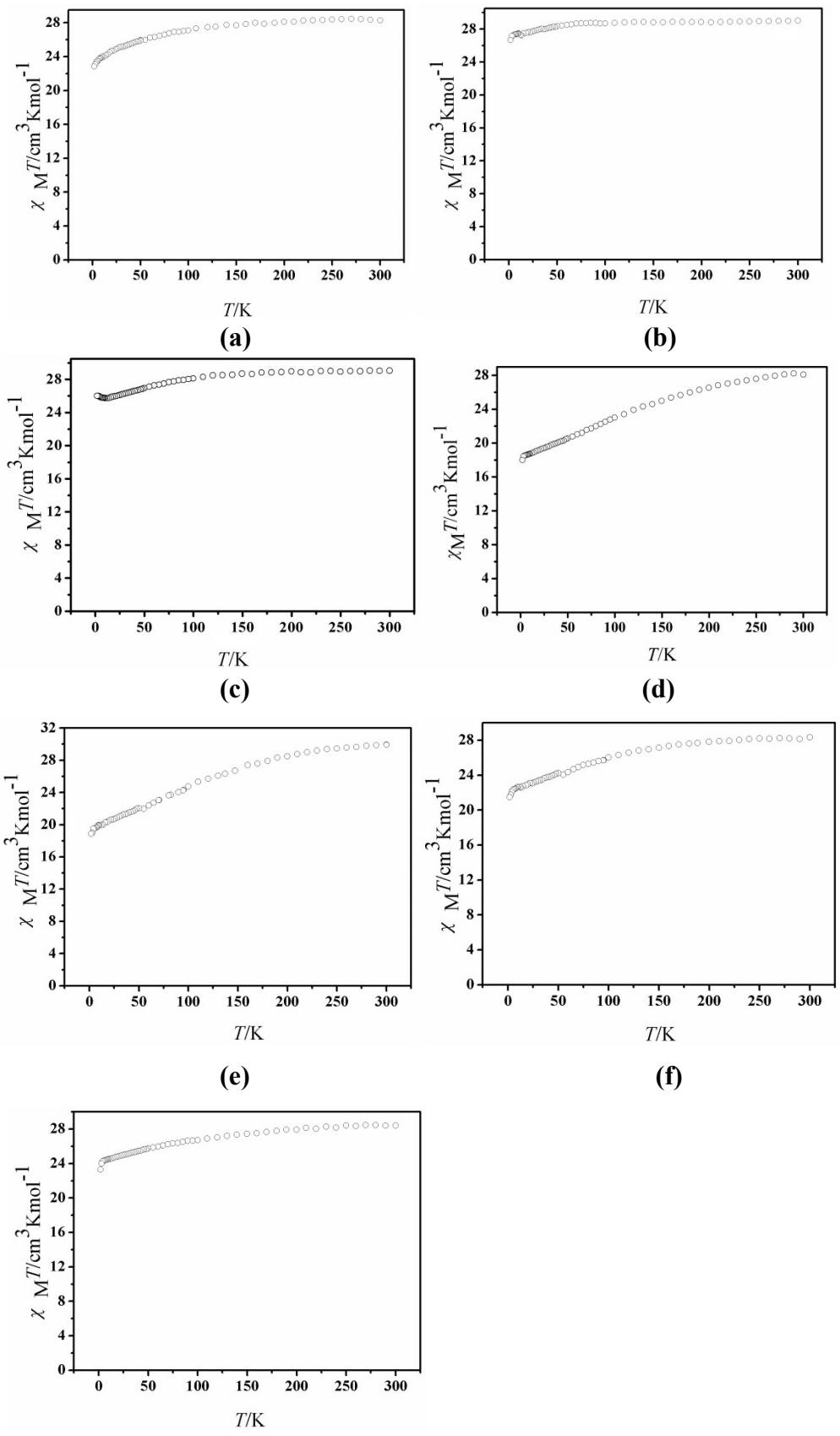

Figure S5. Temperature dependence of $\chi_M T$ measured at 1 KOe for **1-6** (a-g), respectively.

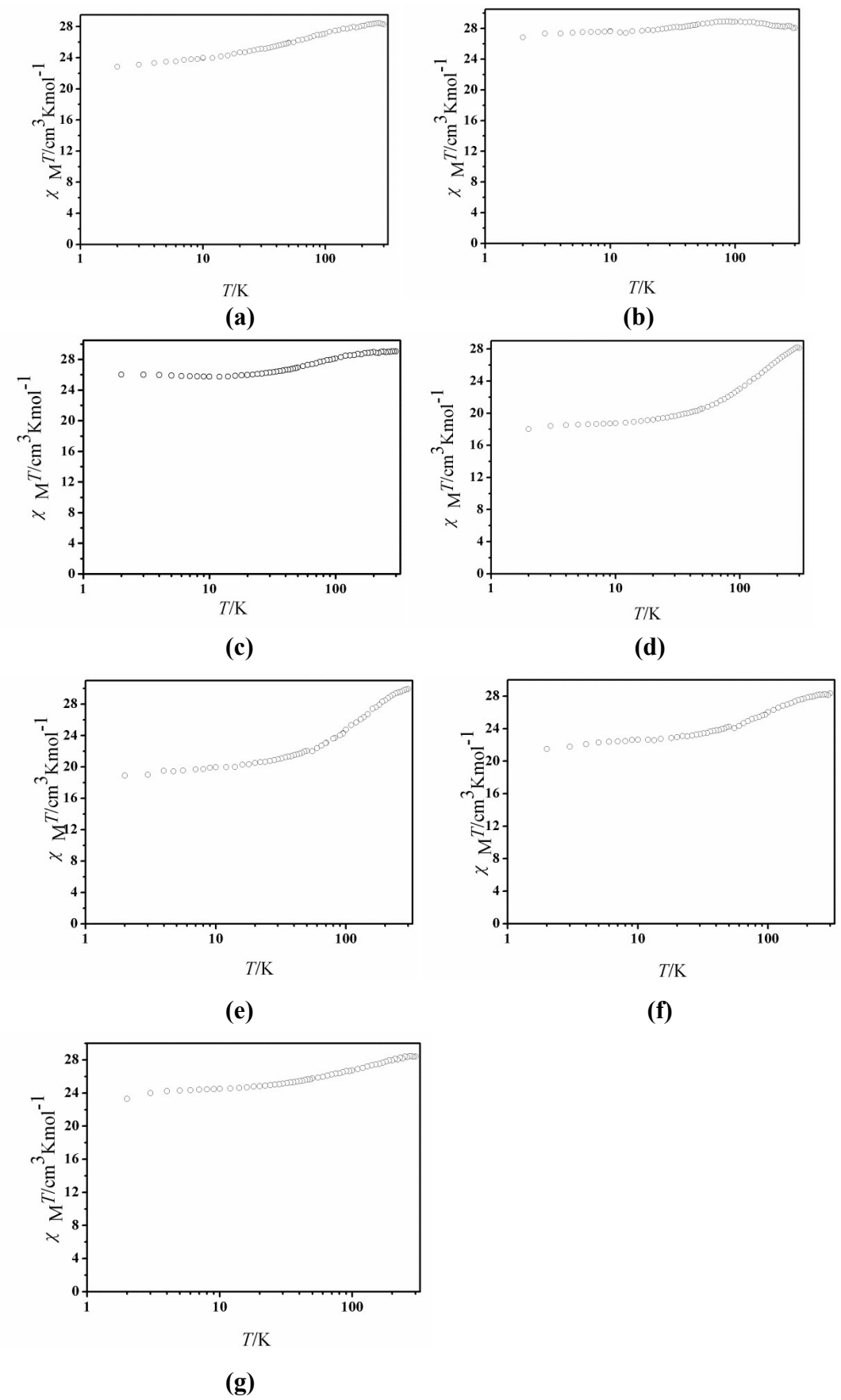

Figure S6. The graphical representations of $\chi_M T$ *vs* *logT* at 1 KOe for **1**-**6** (a-g), respectively.

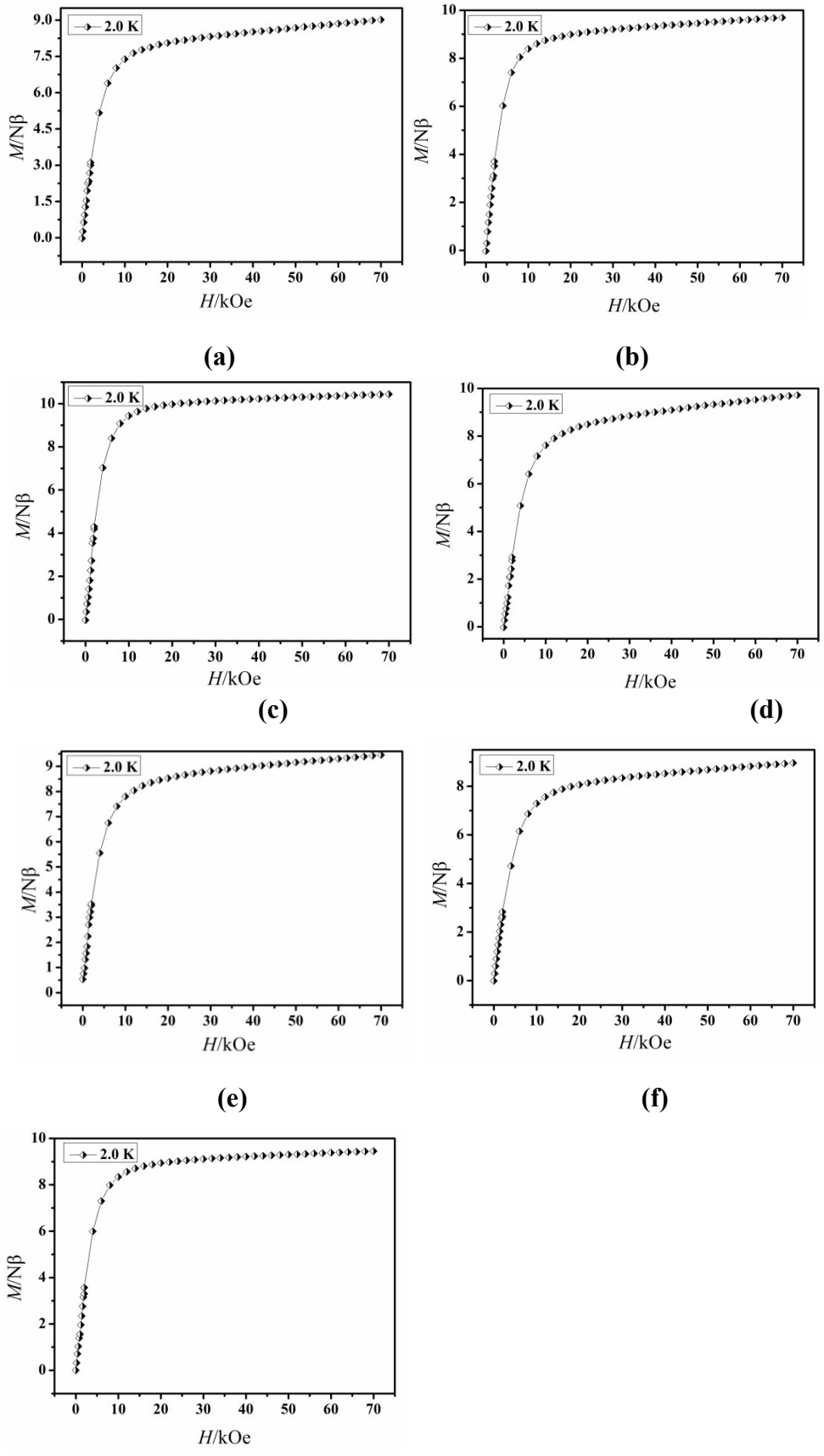

Figure S7. *M*(*H*) plots for **1-6** (a-g), respectively.

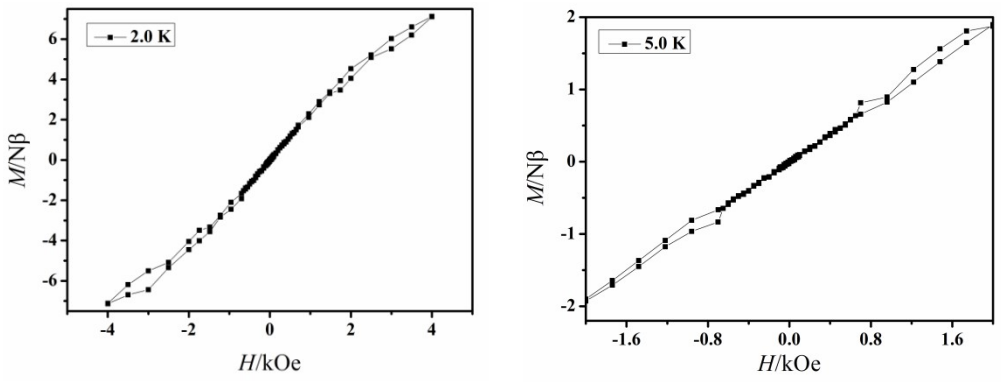

(a) **(b)**

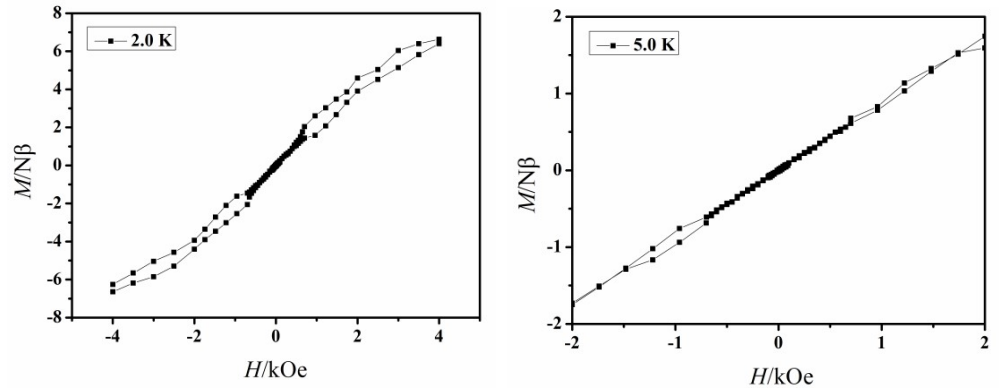

(c) **(d)**

Figure S8. Magnetic hysteresis loops for **2** (a, b) at 2.0 K and 5.0 K. Magnetic hysteresis loops for **3** (c, d) at 2.0 K and 5.0 K.

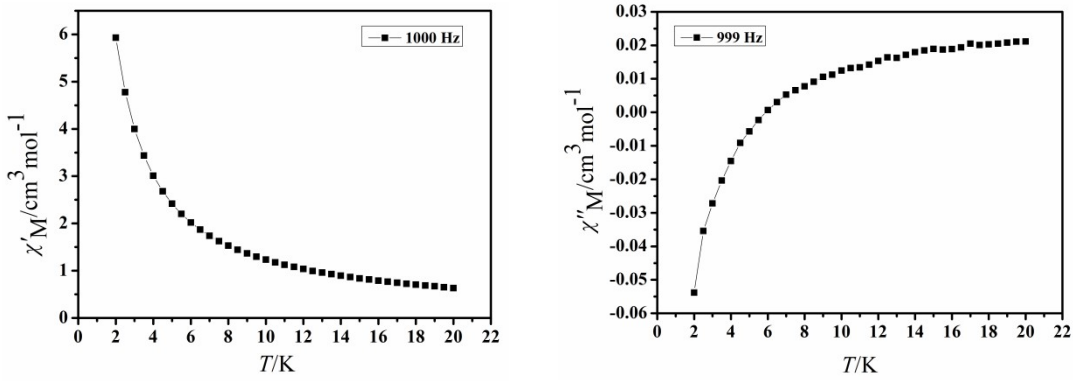

(a) **(b)**

Figure S9. Temperature dependence of the in-phase (χ', a) and out-of-phase (χ'', b) ac susceptibility signals under 0 Oe dc field for **1**.

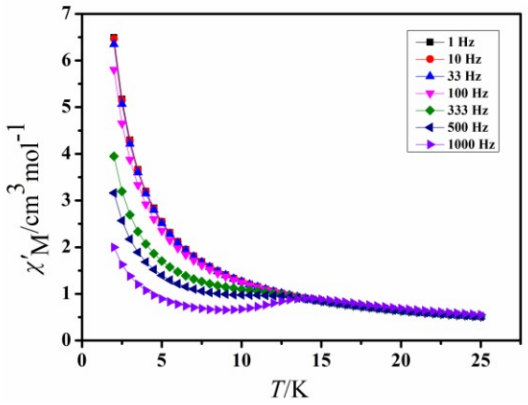

Figure S10. Temperature dependence of the in-phase (χ') ac susceptibility signals under 0 Oe dc field for **2**.

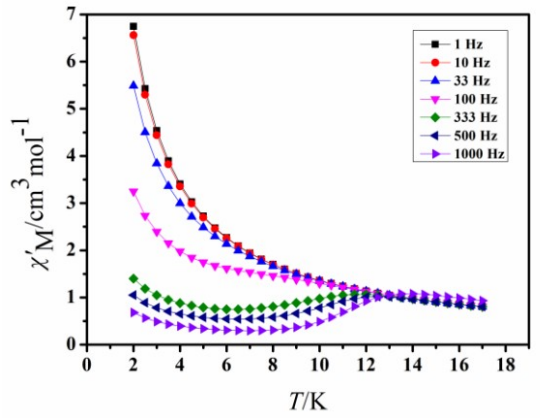

Figure S11. Temperature dependence of the in-phase (χ') ac susceptibility signals under 0 Oe dc field for **3**.

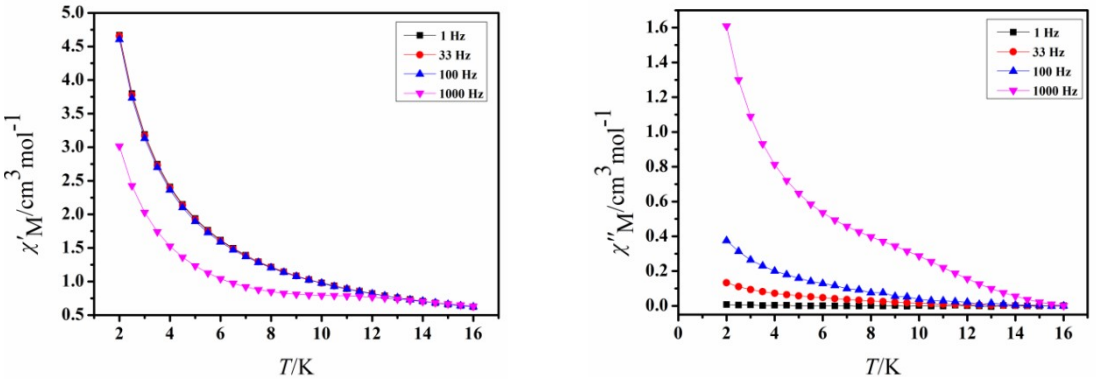

(a) **(b)**

Figure S12. Temperature dependence of the in-phase (χ', a) and out-of-phase (χ'', b) ac susceptibility signals under 0 Oe dc field for **4**.

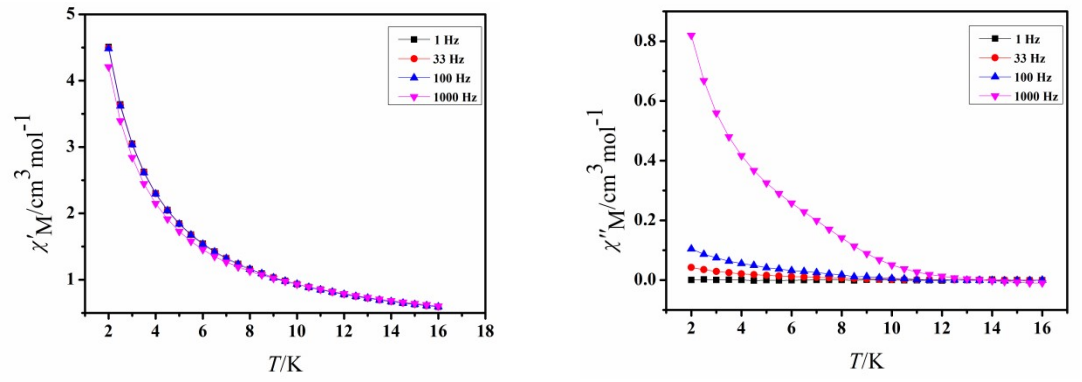

(a) **(b)**

Figure S13. Temperature dependence of the in-phase (χ', a) and out-of-phase (χ'', b) ac susceptibility signals under 0 Oe dc field for **4a**.

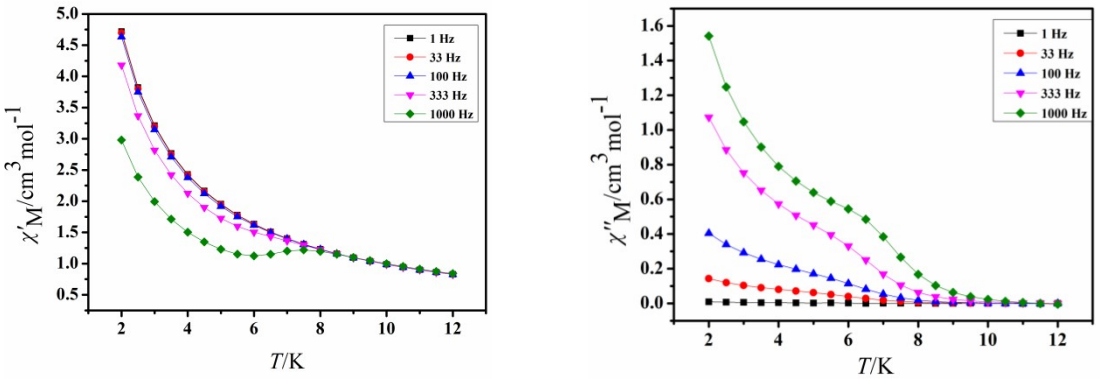

(a) **(b)**

Figure S14. Temperature dependence of the in-phase (χ', a) and out-of-phase (χ'', b) ac susceptibility signals under 0 Oe dc field for **5**.

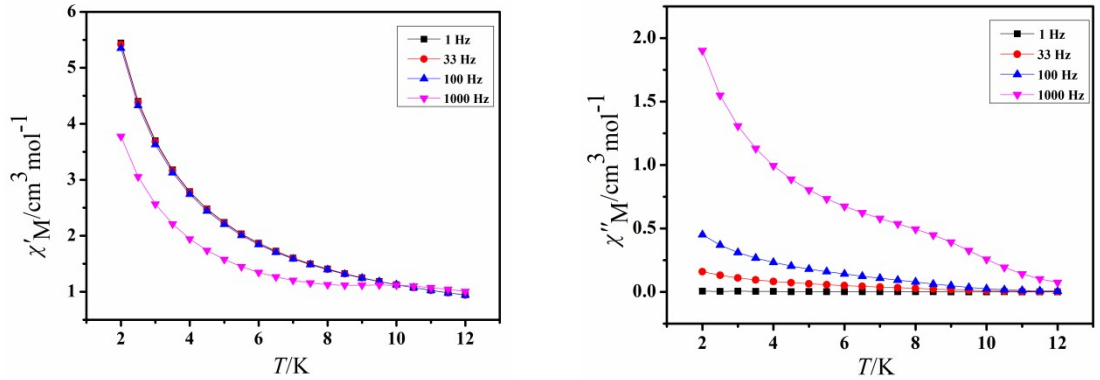

(a) **(b)**

Figure S15. Temperature dependence of the in-phase (χ', a) and out-of-phase (χ'', b) ac susceptibility signals under 0 Oe dc field for **6**.

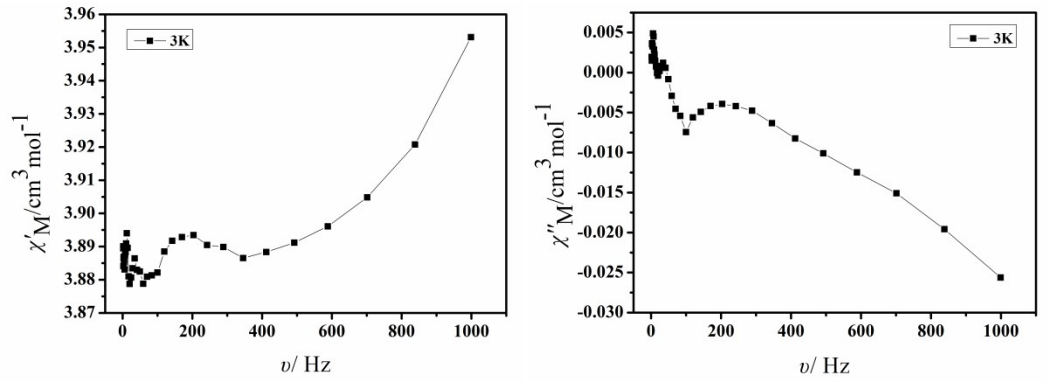

(a) **(b)**

Figure S16. Plots of the frequency-dependent in-phase (χ', a) and out-of-phase (χ'', b) ac susceptibility at 3.0 K for **1** under 0 Oe dc field.

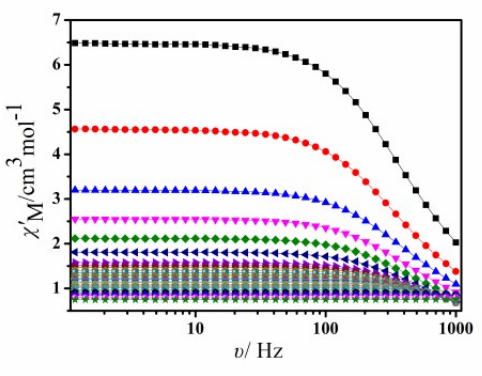

Figure S17. Plots of the frequency-dependent in-phase (χ') ac susceptibility from 2.0 K to 17.0 K for **2** under 0 Oe dc field.

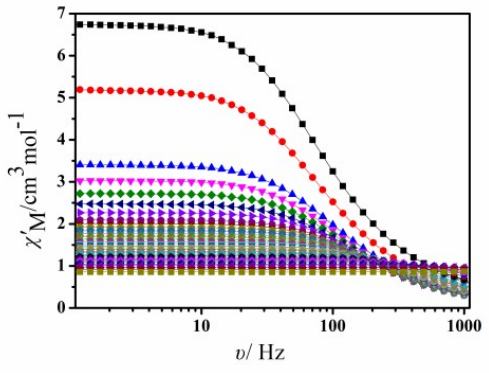

Figure S18. Plots of the frequency-dependent in-phase (χ') ac susceptibility from 2.0 K to 16.0 K for **3** under 0 Oe dc field.

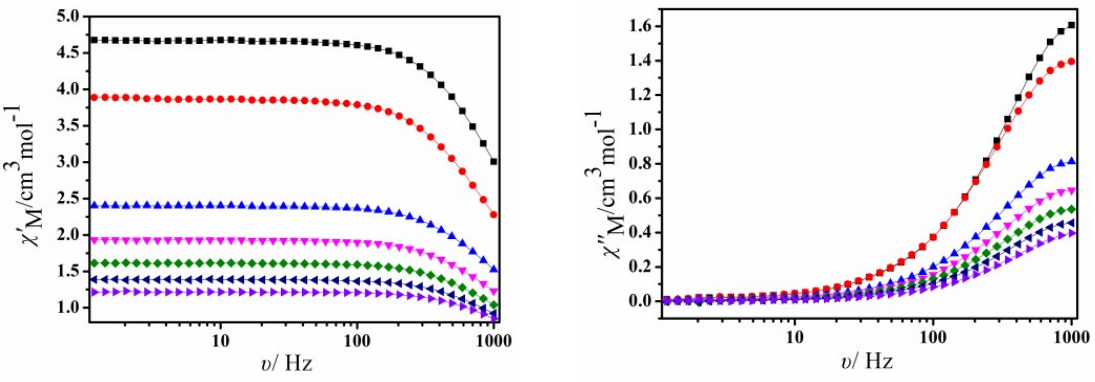

(a) **(b)**

Figure S19. Plots of the frequency-dependent in-phase (χ', a) and out-of-phase (χ'', b) ac susceptibility from 2.0 K to 8.0 K for **4** under 0 Oe dc field.

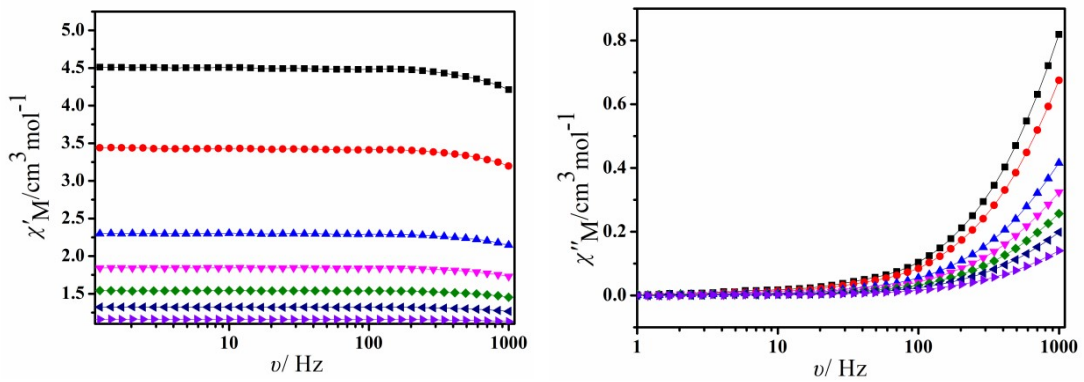

(a) **(b)**

Figure S20. Plots of the frequency-dependent in-phase (χ', a) and out-of-phase (χ'', b) ac susceptibility from 2.0 K to 8.0 K for **4a** under 0 Oe dc field.

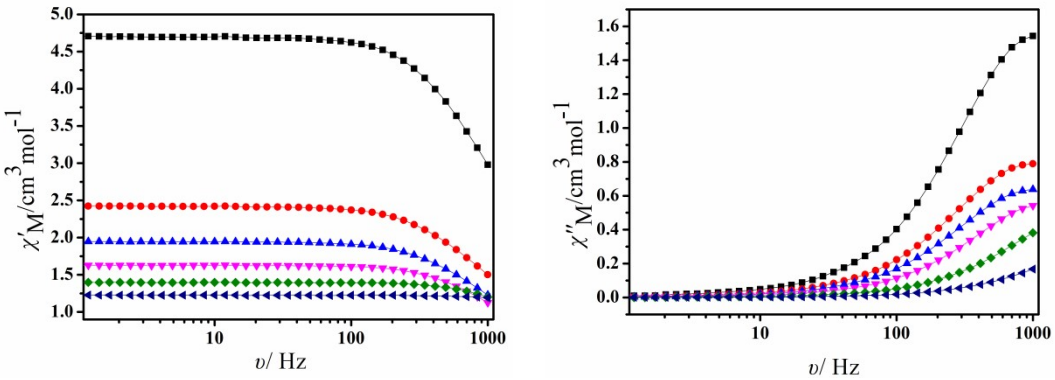

(a) **(b)**

Figure S21. Plots of the frequency-dependent in-phase (χ', a) and out-of-phase (χ'', b) ac susceptibility from 2.0 K to 8.0 K for **5** under 0 Oe dc field.

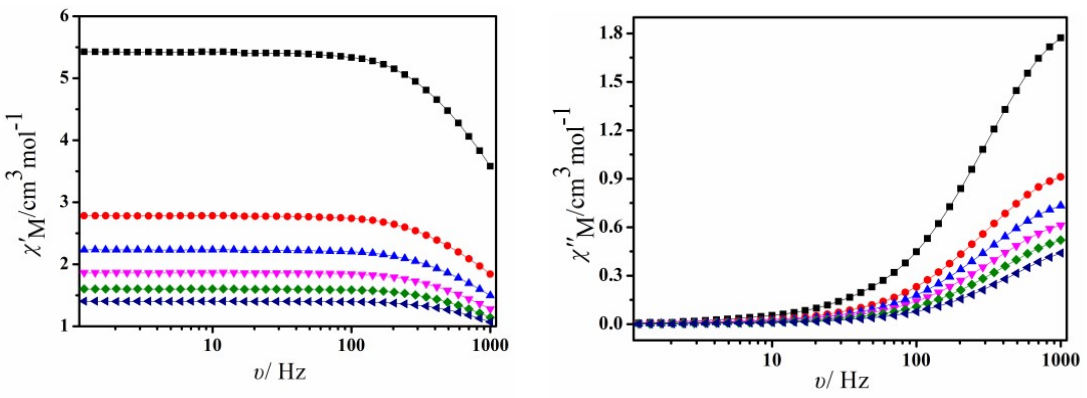

(a) **(b)**

Figure S22. Plots of the frequency-dependent in-phase (χ', a) and out-of-phase (χ'', b) ac susceptibility from 2.0 K to 8.0 K for **6** under 0 Oe dc field.

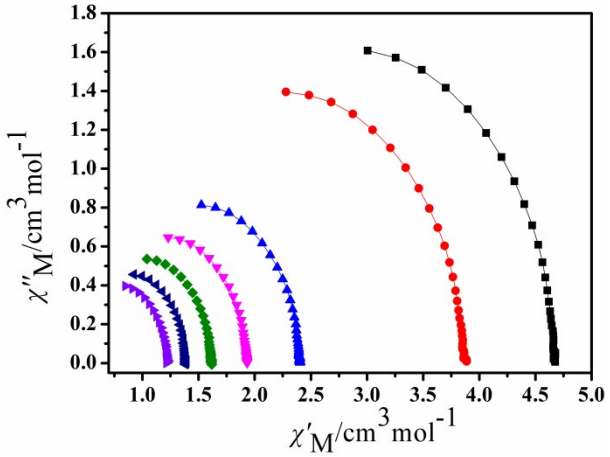

Figure S23. Cole–Cole plots for **4** from 2.0 K to 35.0 K using the ac susceptibility data under a zero applied dc field.

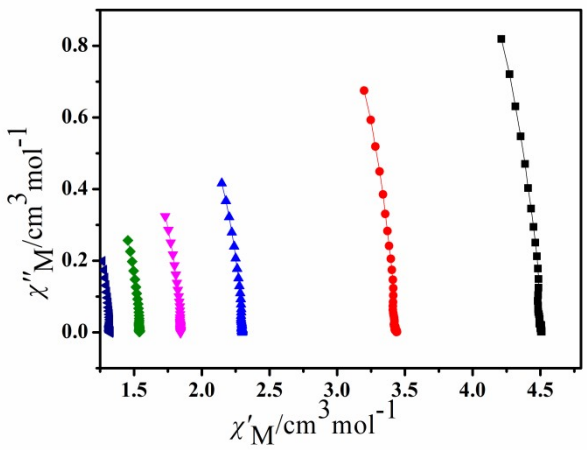

Figure S24. Cole–Cole plots for **4a** from 2.0 K to 8.0 K using the ac susceptibility data under a zero applied dc field.

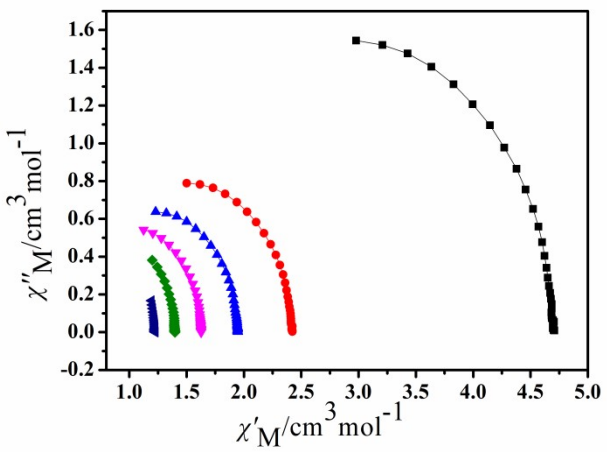

Figure S25. Cole–Cole plots for **5** from 2.0 K to 8.0 K using the ac susceptibility data under a zero applied dc field.

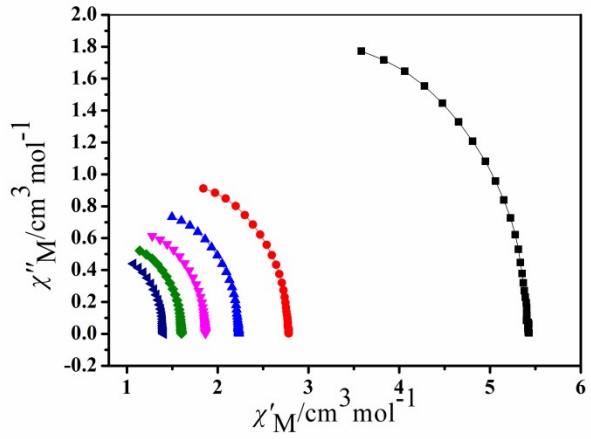

Figure S26. Cole–Cole plots for **6** from 2.0 K to 8.0 K using the ac susceptibility data under a zero applied dc field.

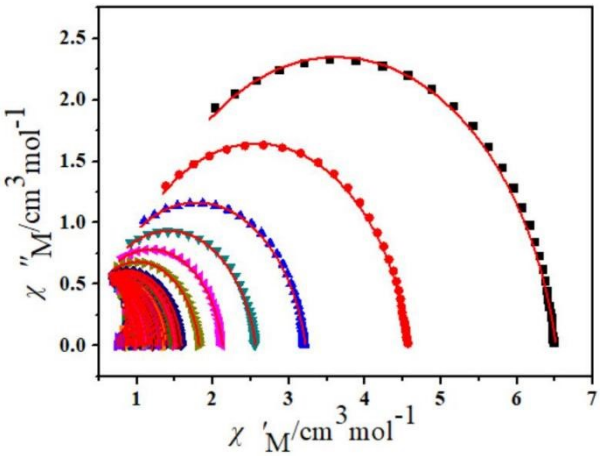

Figure S27. Cole–Cole diagrams with red solid lines as Debye fits for **2**.

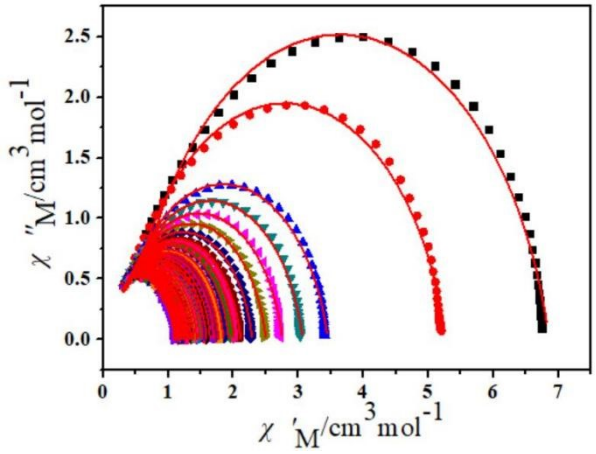

Figure S28. Cole–Cole diagrams with red solid lines as Debye fits for **3**.

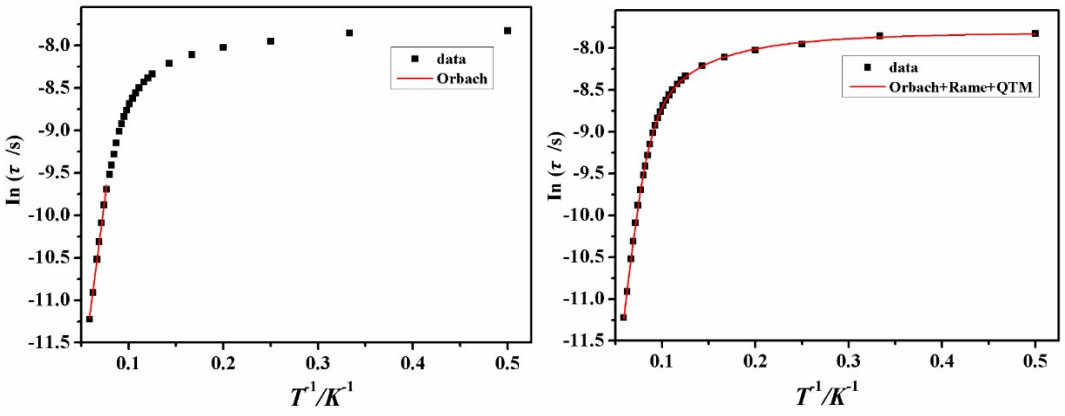

(a) **(b)**

Figure S29. Fitting of frequency dependence of the relaxation time under 0 Oe dc field for **2** (the red line represents the simulation from the Orbach process (a). The red line represents the simulation from the Orbach process, the Raman process, and the QTM process (b)).

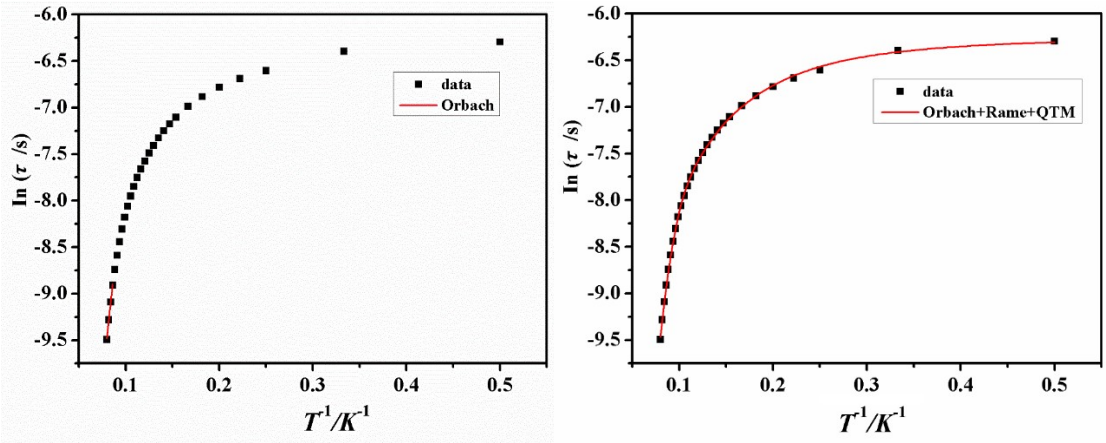

(a) **(b)**

Figure S30. Fitting of frequency dependence of the relaxation time under 0 Oe dc

field for **3** (the red line represents the simulation from the Orbach process (a). The red line represents the simulation from the Orbach process, the Raman process, and the QTM process (b)).

4. Relaxation fitting parameters of 2 and 3

The magnetic susceptibility data of **2** and **3** under a zero dc field were described by the modified Debye functions:

$$\chi'(\omega) = \chi_S + (\chi_T - \chi_S)\frac{1+(\omega\tau)^{1-\alpha}\sin(\frac{\pi}{2}\alpha)}{1+2(\omega\tau)^{1-\alpha}\sin(\frac{\pi}{2}\alpha)+(\omega\tau)^{(2-2\alpha)}}$$

$$\chi''(\omega) = (\chi_T - \chi_S)\frac{(\omega\tau)^{1-\alpha}\cos(\frac{\pi}{2}\alpha)}{1+2(\omega\tau)^{1-\alpha}\sin(\frac{\pi}{2}\alpha)+(\omega\tau)^{(2-2\alpha)}}$$

$$\chi''_{\omega=\tau^{-1}} = (\chi_T - \chi_S)\frac{\cos(\frac{\pi}{2}\alpha)}{2+2\sin(\frac{\pi}{2}\alpha)} = \frac{1}{2}(\chi_T - \chi_S)\tan\frac{\pi}{4}(1-\alpha)$$

Table S4 Relaxation fitting parameters from Least-Squares Fitting of $\chi(\omega)$ data for **2** under a zero applied dc field.

T	$\Delta\chi_1$ (cm^3mol^{-1})	$\Delta\chi_2$ (cm^3mol^{-1})	τ(s)	α	Residual
2.0	0.720264E+00	0.651339E+01	0.399029E-03	0.131169E+00	0.831747E-01
3.0	0.565641E+00	0.457546E+01	0.425420E-03	0.123630E+00	0.283793E-01
4.0	0.351179E+00	0.321591E+01	0.352051E-03	0.129200E+00	0.223842E-01
5.0	0.279196E+00	0.256151E+01	0.327433E-03	0.125259E+00	0.148787E-01
6.0	0.233578E+00	0.212681E+01	0.301291E-03	0.117513E+00	0.104716E-01
7.0	0.198718E+00	0.181870E+01	0.271869E-03	0.107300E+00	0.725481E-02
8.0	0.171400E+00	0.158815E+01	0.239727E-03	0.929873E-01	0.501424E-02
8.3	0.163352E+00	0.153005E+01	0.229269E-03	0.884977E-01	0.436559E-02
8.6	0.155149E+00	0.147589E+01	0.218529E-03	0.839370E-01	0.387075E-02
9.0	0.142441E+00	0.140970E+01	0.203494E-03	0.781917E-01	0.311331E-02
9.3	0.132623E+00	0.136393E+01	0.191874E-03	0.740541E-01	0.265255E-02
9.6	0.122698E+00	0.132082E+01	0.180171E-03	0.697443E-01	0.220855E-02
9.9	0.114929E+00	0.128000E+01	0.168851E-03	0.644825E-01	0.189030E-02
10.2	0.102510E+00	0.124219E+01	0.156716E-03	0.609271E-01	0.148668E-02
10.5	0.937629E-01	0.120645E+01	0.145365E-03	0.557031E-01	0.122852E-02
10.8	0.811590E-01	0.117268E+01	0.133506E-03	0.520722E-01	0.979095E-03

11.1	0.686396E-01	0.114024E+01	0.122002E-03	0.476475E-01	0.790583E-03
11.5	0.461175E-01	0.110081E+01	0.106432E-03	0.442918E-01	0.573836E-03
11.8	0.197048E-01	0.106947E+01	0.934018E-04	0.416611E-01	0.451245E-03
12.2	0.824562E-05	0.104010E+01	0.820472E-04	0.369523E-01	0.338787E-03
12.5	0.170333E-04	0.101207E+01	0.735142E-04	0.279024E-01	0.300853E-03
13.0	0.399060E-04	0.973205E+00	0.615987E-04	0.154149E-01	0.283357E-03
13.5	0.184015E-03	0.936956E+00	0.513077E-04	0.659685E-03	0.249133E-03
14.0	0.381467E-15	0.904341E+00	0.414814E-04	0.840393E-03	0.313150E-03
14.5	0.743667E-27	0.873988E+00	0.333437E-04	0.880874E-03	0.406560E-03
15.0	0.342583E-26	0.845579E+00	0.269959E-04	0.362394E-12	0.454920E-03
16.0	0.363326E-26	0.794745E+00	0.182537E-04	0.527102E-12	0.448304E-03
17.0	0.368928E-26	0.749050E+00	0.133781E-04	0.809549E-12	0.477896E-03

Table S5 Relaxation fitting parameters from Least-Squares Fitting of $\chi(\omega)$ data for **3** under a zero applied dc field.

T	$\Delta\chi_1$ (cm^3mol^{-1})	$\Delta\chi_2$ (cm^3mol^{-1})	τ(s)	α	Residual
2.0	0.428704E+00	0.685635E+01	0.184866E-02	0.152917E+00	0.319732E+00
3.0	0.317708E+00	0.526941E+01	0.180804E-02	0.149731E+00	0.183227E+00
4.0	0.228177E+00	0.345440E+01	0.135615E-02	0.144159E+00	0.725343E-01
4.5	0.205991E+00	0.306722E+01	0.124376E-02	0.138392E+00	0.538761E-01
5.0	0.187729E+00	0.275576E+01	0.113343E-02	0.131245E+00	0.399342E-01
5.5	0.172183E+00	0.250103E+01	0.102614E-02	0.123182E+00	0.294102E-01
6.0	0.158557E+00	0.228926E+01	0.922380E-03	0.114730E+00	0.213619E-01
6.5	0.146339E+00	0.210969E+01	0.822705E-03	0.106089E+00	0.153356E-01
6.8	0.139394E+00	0.201479E+01	0.765139E-03	0.101121E+00	0.123048E-01
7.1	0.132676E+00	0.192856E+01	0.710178E-03	0.964143E-01	0.999783E-02
7.4	0.126882E+00	0.184944E+01	0.657647E-03	0.915861E-01	0.812206E-02
7.7	0.121745E+00	0.177622E+01	0.607228E-03	0.867710E-01	0.671546E-02
8.0	0.117198E+00	0.170878E+01	0.559515E-03	0.822556E-01	0.548492E-02
8.3	0.113186E+00	0.164608E+01	0.513930E-03	0.778933E-01	0.450543E-02
8.6	0.109597E+00	0.158813E+01	0.470683E-03	0.739194E-01	0.371441E-02
8.9	0.107141E+00	0.153395E+01	0.429529E-03	0.702284E-01	0.307819E-02
9.2	0.104471E+00	0.148333E+01	0.389850E-03	0.671518E-01	0.251915E-02
9.5	0.103191E+00	0.143659E+01	0.352132E-03	0.645784E-01	0.200025E-02
9.8	0.103037E+00	0.139189E+01	0.315695E-03	0.619033E-01	0.177422E-02
10.1	0.103682E+00	0.135053E+01	0.280730E-03	0.598122E-01	0.147618E-02
10.4	0.105468E+00	0.131166E+01	0.247252E-03	0.585174E-01	0.118864E-02
10.7	0.110808E+00	0.127464E+01	0.215873E-03	0.567659E-01	0.104480E-02
11.0	0.117343E+00	0.123982E+01	0.186464E-03	0.552513E-01	0.856482E-03
11.3	0.127842E+00	0.120662E+01	0.159732E-03	0.532719E-01	0.718128E-03
11.6	0.138174E+00	0.117529E+01	0.135046E-03	0.518116E-01	0.628180E-03
11.9	0.147869E+00	0.114569E+01	0.112838E-03	0.509334E-01	0.479482E-03
12.2	0.156143E+00	0.111745E+01	0.930475E-04	0.502283E-01	0.404931E-03

12.5	0.158213E+00	0.109052E+01	0.754524E-04	0.499730E-01	0.310396E-03
13.0	0.126060E+00	0.104887E+01	0.497286E-04	0.523226E-01	0.185403E-03
13.5	0.215981E-11	0.101022E+01	0.288732E-04	0.541410E-01	0.139207E-03
14.0	0.329664E-11	0.910246E+00	0.970678E-05	0.335225E-15	0.171006E-03
15.0	0.595189E-11	0.856111E+00	0.419926E-05	0.457149E-15	0.312791E-03
16.0	0.595213E-11	0.856111E+00	0.419926E-05	0.685686E-15	0.312791E-03

Theoretical methods and computational details:

Multiconfigurational *ab initio* calculations, including spin-orbit coupling (SOC), were performed on the experimental structures of the complexes here to explore their SMM propertiesy. This type of calculation includes two steps:[1] 1) a set of spin eigenstates, are obtained by the state-averaged (SA) CASSCF method;[2] 2) the low-lying SOC states, i.e., Kramers doublets (KD) herein, are obtained by state interaction which is the diagonalization of the SOC matrix in the space spanned by the spin eigenstates from the first step. In the CASSCF step, the active space consisted of 9 electrons in 7 orbitals and all the spin eigenstates of 21 sextets were included. Due to the hardware limitation, other highly excited quartets and doublets were not considered. The step of state interaction were performed by the RASSI-SO module [3] with the SOC integrals from the AMFI method.[4] The ANO-RCC basis sets,[5–7] including VTZP for Dy and Lu, VDZ for C and H as well as VDZP for other atoms, were used. All the calculations were carried out with the MOLCAS@UU, a version of MOLCAS 8.0[10,11] which is freely distributed for academic users. The SINGLE ANISO module [8,9] developed by Chibotaru and et al, was used to obtain the *g*-tensors, transition magnetic moments and other parameters characterizing the magnetic anisotropy.

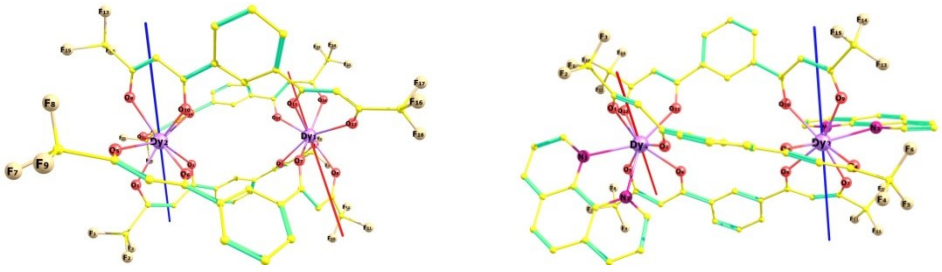

(a) **(b)**

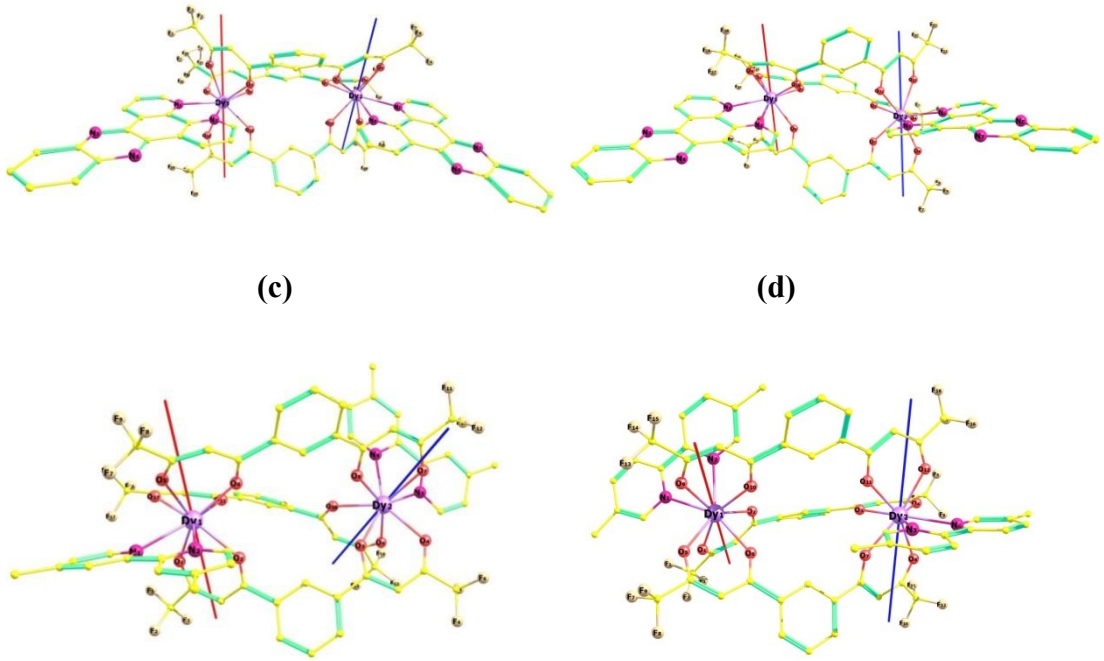

(c) **(d)**

(e) **(f)**

Figure S31. The *ab initio* magnetic easy axes of the two Dy^{III} of **1** (a)**, 2** (b)**, 4** (c)**, 4a** (d)**, 5** (e) and **6** (f).

Table S6 Calculated energy levels (cm^{-1}), ***g*** (g_x, g_y, g_z) tensors of the lowest eight KDs of individual Dy^{III} fragments of complexes **1-6** using CASSCF/RASSI-SO with MOLCAS 8.2.

1-a	KD_0	KD_1	KD_2	KD_3	KD_4	KD_5	KD_6	KD_7
g_X	4.027E-01	4.674E-01	3.789E-02	1.679E+00	1.045E+00	1.082E+00	1.979E-02	1.315E-04
g_Y	4.217E+00	3.713E+00	7.729E-01	4.312E+00	6.078E+00	6.794E+00	1.118E-01	8.580E-04
g_Z	1.606E+01	1.552E+01	1.661E+01	1.116E+01	7.204E+00	1.247E+01	1.721E+01	1.994E+01
g_{XY}	4.236E+00	3.742E+00	7.738E-01	4.627E+00	6.167E+00	6.879E+00	1.136E-01	8.681E-04
E(KD) cm^{-1}	0.000E+00	1.669E+01	1.547E+02	1.631E+02	1.776E+02	1.949E+02	2.512E+02	6.740E+02
1-b	KD_0	KD_1	KD_2	KD_3	KD_4	KD_5	KD_6	KD_7
g_X	1.146E-01	1.184E-01	1.368E+00	2.585E+00	3.123E+00	3.613E-01	5.339E-02	1.606E-04
g_Y	4.333E-01	3.207E-01	2.071E+00	4.570E+00	5.328E+00	6.392E-01	1.008E+00	1.313E-03
g_Z	1.957E+01	1.932E+01	1.678E+01	1.179E+01	1.171E+01	1.747E+01	1.618E+01	1.994E+01
g_{XY}	4.482E-	3.418E-	2.482E	5.250E	6.176E	7.342E-	1.009E	1.323E-

	01	01	+00	+00	+00	01	+00	03
E(KD) cm^{-1}	0.000E+00	3.984E+01	1.487E+02	1.693E+02	1.866E+02	2.309E+02	2.537E+02	6.712E+02
2-a	KD_0	KD_1	KD_2	KD_3	KD_4	KD_5	KD_6	KD_7
g_X	3.349E-02	7.197E-01	1.028E+00	7.751E+00	2.894E-01	1.075E+00	1.546E-01	1.151E-02
g_Y	5.822E-02	1.465E+00	1.309E+00	4.648E+00	1.758E+00	1.813E+00	3.554E-01	2.678E-02
g_Z	1.960E+01	1.748E+01	1.150E+01	8.323E+00	1.347E+01	1.571E+01	1.874E+01	1.972E+01
g_{XY}	6.717E-02	1.632E+00	1.664E+00	9.038E+00	1.781E+00	2.107E+00	3.875E-01	2.915E-02
E(KD) cm^{-1}	0.000E+00	8.694E+01	1.341E+02	1.606E+02	2.011E+02	2.461E+02	3.207E+02	4.460E+02
2-b	KD_0	KD_1	KD_2	KD_3	KD_4	KD_5	KD_6	KD_7
g_X	3.348E-02	7.202E-01	1.027E+00	7.755E+00	2.906E-01	1.073E+00	1.543E-01	1.140E-02
g_Y	5.823E-02	1.465E+00	1.310E+00	4.647E+00	1.758E+00	1.811E+00	3.542E-01	2.674E-02
g_Z	1.959E+01	1.749E+01	1.151E+01	8.323E+00	1.348E+01	1.569E+01	1.873E+01	1.973E+01
g_{XY}	6.717E-02	1.633E+00	1.664E+00	9.040E+00	1.781E+00	2.105E+00	3.863E-01	2.907E-02
E(KD) cm^{-1}	0.000E+00	8.694E+01	1.341E+02	1.606E+02	2.011E+02	2.461E+02	3.207E+02	4.460E+02
3-a	KD_0	KD_1	KD_2	KD_3	KD_4	KD_5	KD_6	KD_7
g_X	4.999E-03	8.130E-01	4.048E+00	1.964E+00	3.136E-01	1.215E-01	2.003E-02	4.642E-03
g_Y	1.208E-02	1.550E+00	5.479E+00	2.297E+00	9.201E-01	1.497E-01	8.880E-02	9.270E-03
g_Z	1.953E+01	1.540E+01	1.065E+01	9.700E+00	1.340E+01	1.744E+01	1.928E+01	1.984E+01
g_{XY}	1.308E-02	1.751E+00	6.812E+00	3.022E+00	9.721E-01	1.928E-01	9.103E-02	1.037E-02
E(KD) cm^{-1}	0.000E+00	1.229E+02	1.616E+02	1.897E+02	2.292E+02	2.805E+02	3.422E+02	4.741E+02
3-b	KD_0	KD_1	KD_2	KD_3	KD_4	KD_5	KD_6	KD_7
g_X	1.576E-02	1.453E+00	2.584E+00	2.073E+00	2.501E-01	9.984E-01	1.140E-01	2.640E-02
g_Y	1.994E-02	5.405E+00	6.971E+00	4.410E+00	3.089E+00	1.697E+00	4.238E-01	7.670E-02
g_Z	1.956E+01	1.296E+01	9.306E+00	1.034E+01	1.335E+01	1.724E+01	1.889E+01	1.959E+01

g_{XY}	2.541E-02	5.597E+00	7.434E+00	4.873E+00	3.100E+00	1.968E+00	4.389E-01	8.112E-02
E(KD) cm^{-1}	0.000E+00	1.345E+02	1.544E+02	1.852E+02	2.408E+02	2.834E+02	3.648E+02	4.491E+02
4-a	KD_0	KD_1	KD_2	KD_3	KD_4	KD_5	KD_6	KD_7
g_X	1.333E-02	8.927E-01	1.947E-01	2.489E+00	2.457E+00	2.080E-02	1.572E-01	1.911E-02
g_Y	2.338E-02	1.209E+00	1.474E+00	3.953E+00	6.051E+00	7.566E-01	5.334E-01	3.897E-02
g_Z	1.935E+01	1.459E+01	1.068E+01	1.498E+01	1.127E+01	1.727E+01	1.834E+01	1.986E+01
g_{XY}	2.691E-02	1.503E+00	1.487E+00	4.671E+00	6.531E+00	7.569E-01	5.560E-01	4.340E-02
E(KD) cm^{-1}	0.000E+00	1.176E+02	1.620E+02	1.880E+02	2.034E+02	2.865E+02	3.168E+02	4.566E+02
4-b	KD_0	KD_1	KD_2	KD_3	KD_4	KD_5	KD_6	KD_7
g_X	1.215E-02	8.263E-01	3.543E-01	2.873E+00	2.073E+00	6.248E-03	1.595E-01	1.878E-02
g_Y	2.147E-02	1.147E+00	1.560E+00	4.179E+00	5.453E+00	7.635E-01	5.484E-01	3.832E-02
g_Z	1.936E+01	1.467E+01	1.085E+01	1.444E+01	1.150E+01	1.726E+01	1.835E+01	1.985E+01
g_{XY}	2.467E-02	1.414E+00	1.599E+00	5.071E+00	5.834E+00	7.635E-01	5.711E-01	4.267E-02
E(KD) cm^{-1}	0.000E+00	1.197E+02	1.654E+02	1.944E+02	2.080E+02	2.906E+02	3.209E+02	4.610E+02
4a-a	KD_0	KD_1	KD_2	KD_3	KD_4	KD_5	KD_6	KD_7
g_X	3.063E-02	1.072E+00	4.353E-01	3.775E+00	3.185E-01	9.729E-01	2.278E-01	2.940E-02
g_Y	3.509E-02	1.364E+00	2.235E+00	4.820E+00	2.883E+00	1.222E+00	4.865E-01	7.565E-02
g_Z	1.952E+01	1.581E+01	1.119E+01	1.029E+01	1.243E+01	1.795E+01	1.886E+01	1.973E+01
g_{XY}	4.657E-02	1.735E+00	2.277E+00	6.123E+00	2.901E+00	1.562E+00	5.372E-01	8.116E-02
E(KD) cm^{-1}	0.000E+00	1.153E+02	1.568E+02	1.855E+02	2.218E+02	2.715E+02	3.573E+02	4.867E+02
4a-b	KD_0	KD_1	KD_2	KD_3	KD_4	KD_5	KD_6	KD_7
g_X	4.323E-02	1.093E+00	4.090E+00	1.977E-01	1.067E+00	1.101E+00	1.704E-01	8.889E-02
g_Y	8.943E-02	3.217E+00	5.357E+00	2.568E+00	2.544E+00	3.596E+00	2.544E-01	3.789E-01
g_Z	1.944E	1.529E	9.210E	1.223E	1.204E	1.417E	1.820E	1.865E

	+01	+01	+00	+01	+01	+01	+01	+01
g_{XY}	9.934E-02	3.398E+00	6.740E+00	2.576E+00	2.759E+00	3.761E+00	3.062E-01	3.892E-01
E(KD) cm^{-1}	0.000E+00	9.773E+01	1.391E+02	1.701E+02	2.130E+02	2.465E+02	4.130E+02	4.563E+02
5-a	KD_0	KD_1	KD_2	KD_3	KD_4	KD_5	KD_6	KD_7
g_X	3.207E-02	4.853E-01	2.904E+00	4.486E+00	2.523E-01	2.127E-01	2.949E-02	5.097E-03
g_Y	6.408E-02	1.339E+00	3.326E+00	5.530E+00	7.544E-01	3.469E-01	5.792E-02	1.543E-02
g_Z	1.954E+01	1.777E+01	1.272E+01	9.764E+00	1.439E+01	1.677E+01	1.926E+01	1.975E+01
g_{XY}	7.165E-02	1.425E+00	4.415E+00	7.121E+00	7.955E-01	4.069E-01	6.500E-02	1.625E-02
E(KD) cm^{-1}	0.000E+00	8.327E+01	1.207E+02	1.523E+02	1.920E+02	2.462E+02	3.138E+02	4.045E+02
5-b	KD_0	KD_1	KD_2	KD_3	KD_4	KD_5	KD_6	KD_7
g_X	3.203E-02	4.851E-01	2.902E+00	4.484E+00	2.525E-01	2.124E-01	2.969E-02	4.998E-03
g_Y	6.410E-02	1.340E+00	3.327E+00	5.531E+00	7.542E-01	3.462E-01	5.824E-02	1.542E-02
g_Z	1.953E+01	1.778E+01	1.274E+01	9.765E+00	1.439E+01	1.676E+01	1.925E+01	1.975E+01
g_{XY}	7.165E-02	1.425E+00	4.414E+00	7.121E+00	7.954E-01	4.062E-01	6.537E-02	1.621E-02
E(KD) cm^{-1}	0.000E+00	8.326E+01	1.207E+02	1.523E+02	1.920E+02	2.462E+02	3.138E+02	4.045E+02
6-a	KD_0	KD_1	KD_2	KD_3	KD_4	KD_5	KD_6	KD_7
g_X	4.753E-03	4.829E-01	3.385E+00	1.506E+00	1.806E-01	9.011E-01	1.731E-01	8.953E-02
g_Y	4.506E-02	1.865E+00	4.847E+00	5.175E+00	1.824E+00	2.065E+00	4.928E-01	6.331E-01
g_Z	1.944E+01	1.711E+01	9.652E+00	1.124E+01	1.390E+01	1.585E+01	1.762E+01	1.807E+01
g_{XY}	4.531E-02	1.926E+00	5.912E+00	5.389E+00	1.833E+00	2.253E+00	5.223E-01	6.394E-01
E(KD) cm^{-1}	0.000E+00	7.281E+01	1.203E+02	1.483E+02	1.887E+02	2.320E+02	3.861E+02	4.185E+02
6-b	KD_0	KD_1	KD_2	KD_3	KD_4	KD_5	KD_6	KD_7
g_X	2.880E-02	9.654E-01	9.289E-01	3.698E+00	1.236E+00	5.092E-01	7.397E-01	3.549E-01
g_Y	5.044E-02	2.624E+00	4.400E+00	5.429E+00	2.667E+00	8.448E-01	5.763E+00	6.468E+00

g_Z	1.956E+01	1.710E+01	1.202E+01	1.011E+01	1.495E+01	1.814E+01	1.273E+01	1.332E+01
g_{XY}	5.808E-02	2.796E+00	4.497E+00	6.569E+00	2.940E+00	9.864E-01	5.810E+00	6.477E+00
E(KD) cm^{-1}	0.000E+00	1.167E+02	1.491E+02	1.822E+02	2.454E+02	3.123E+02	4.257E+02	4.461E+02

Table S7 Angle θ with Respect to the *ab initio* Magnetic Easy Axis (in °), Distance R to Central Dy^{3+} (in Å), Atomic Charge Q (in e) of the Atoms in the First Sphere of **1**.

1-Dy^{III}-a	θ	R	Q	**1-Dy^{III}-b**	*θ*	R	Q
O	34.3	2.347	-0.691	O	33.9	2.361	-0.682
O	35.4	2.362	-0.679	O	34.8	2.352	-0.700
O	37.7	2.337	-0.665	O	39.3	2.317	-0.672
O	39.7	2.321	-0.692	O	39.6	2.329	-0.665
O	72.1	2.315	-0.689	O	72.4	2.355	-0.657
O	73.5	2.399	-0.666	O	73.0	2.327	-0.684
O	74.2	2.330	-0.703	O	74.6	2.338	-0.671
O	76.1	2.342	-0.653	O	74.6	2.393	-0.682

Table S8 Angle θ with Respect to the *ab initio* Magnetic Easy Axis (in °), Distance R to Central Dy^{3+} (in Å), Atomic Charge Q (in e) of the Atoms in the First Sphere of **3**.

3-Dy^{III}-a	*θ*	R	Q	**3-Dy^{III}-b**	*θ*	R	Q
O	17.4	2.333	-0.716	O	23.1	2.332	-0.669
O	29.7	2.335	-0.704	O	24.6	2.298	-0.696
O	42.5	2.311	-0.693	O	47.9	2.303	-0.695
O	59.9	2.352	-0.688	O	50.7	2.363	-0.714
O	75.7	2.307	-0.711	O	81.9	2.329	-0.699
O	79.4	2.316	-0.690	O	83.2	2.313	-0.699
N	83.6	2.569	-0.352	O	86.3	2.539	-0.345
N	87.6	2.534	-0.345	O	87.1	2.543	-0.346

References:

(1) J. Luzon, R. Sessoli, *Dalton Trans.,* 2012, **41**, 13556–13567.

(2) B. O. Roos, P. R. Taylor, P. E. M. Siegbahn, *Chem. Phys.,* 1980, **48**, 157–173.

(3) P. Malmqvist, B. O. Roos, B. Schimmelpfennig, *Chem. Phys. Lett.,* 2002, **357**, 230–240.

(4) B. A. Hess, C. M. Marian, U.Wahlgren, O. Gropen, *Chem. Phys. Lett.,* 1996, **251**, 365–371.

(5) B. O. Roos, R. Lindh, P. Malmqvist, V. Veryazov, P. Widmark, *J. Phys. Chem. A.,* 2004, **108**, 2851–2858.

(6) B. O. Roos, R. Lindh, P. Malmqvist, V.Veryazov, P. Widmark, *J. Phys. Chem. A.,*

2005, **109**, 6575–6579.

(7) B. O. Roos, R. Lindh, P. Malmqvist, V. Veryazov, P. Widmark, A. C. Borin, *J. Phys. Chem. A.,* 2008, **112**, 11431–11435.

(8) L. F. Chibotaru, L. Ungur, *J. Chem. Phys.,* 2012, **137**, 064112.

(9) L. F. Chibotaru, *Adv. Chem. Phys.,* 2013, **153**, 397–519.

(10) F. Aquilante, L. De Vico, N. Ferre, G. Ghigo, P. A. Malmqvist, P. Neograd y, T. B. Pedersen, M. Pitonak, M. Reiher, B. O. Roos, L. Serrano-Andres, M. Urban, V. Veryazov, R. Lindh, *Molcas 7: The next generation*. 2010, **31**, 224–247.

(11) F. Aquilante, J. Autschbach, R. K. Carlson, L. F. Chibotaru, M. G. Delcey, L. D. Vico, I. F. Galvan, N. Ferre, L. M. Frutos, L. Gagliardi, M. Garavelli, A. Giussani, C. E. Hoyer, G. L. Manni, H. Lischka, D. Ma, P. A. Malmqvist, T. Muller, A. Nenov, M. Olivucci, T. B. Pedersen, D. Peng, F. Plasser, B. Pritchard, M. Reiher, I. Rivalta, I. Schapiro, J. Segarra-Marti, M. Stenrup, D. G. Truhlar, L. Ungur, A. Valentini, S. Vancoillie, V. Veryazov, V. P. Vysotskiy, O. Weingart, F. Zapata, R. Lindh, *J. Comput. Chem.,* 2016, **37**, 506–541.